

The Unification of the Pole Placement and Linear Quadratic Gaussian Techniques

Demetrios Matsakis
U.S. Naval Observatory, Washington DC, USA

Abstract

Two approaches to steering clocks to a reference standard via frequency steers have been explored in the literature, the Linear Quadratic Gaussian (LQG) approach and the Pole Placement (PP) approach. LQG minimizes a user-selected cost function, which is a linear combination of the expected variances of the phase, frequency, and control effort (frequency steers). The PP method sets the response time of the controlled clock. We unify these techniques by developing an analysis that quantifies what time constants are in fact determined by LQG-derived gains, and what total costs would be incurred under PP-derived gains. We also explore the effects of suboptimal state estimation, and of delays between the time measurements are made and when the steering decisions based upon them are incorporated into the system.

Introduction

Control theory is often taught at the graduate level, and appears in generalized form in textbooks and publications such as [1-4]. These approaches have been applied to disciplining oscillators [5,6]. The theory is not yet complete because it does not fully address the effects of small variations in the loop gains, suboptimal modelling, and other properties [7,8], although simulations [9] can provide a useful supplement in this regard.

This paper extends published analyses of the PP and LQG techniques [5], which are capable of finding the gains that optimize performance as defined by either the time constants or by a linear combination of the phase, frequency, and control variances respectively. We unify the two techniques by deriving the formulas to compute the variances and time constants when the gains are at the desired value, as well as for any other values that do not result in unbounded performance. Unfortunately, it is not always possible to correctly or even optimally estimate the state, and in some systems there may be long delays before a steer can be implemented. We therefore derive formulas to quantify the effects of suboptimal state estimation when measurement noise is ignored, and for data processing lags.

A key concept is the Separation Theorem, which states that the optimal control strategy is independent of the optimal state estimate method. Therefore, the optimal control parameters can be derived without reference to the noise of the measurements, or the intrinsic variation of the state function. We follow the Kalman formalism for state estimation since it can be shown that it yields an optimal estimate of the current state, if properly parameterized and if the noise contributions are independent.

Although a variety of control schemes are possible, we consider only those in which the clock is controlled by shifting its frequency as fractions (gains) of its phase and frequency deviations from the reference standard; typical examples are a laboratory timescale steered to Coordinated Universal Time (UTC), or a precise clock steered to a local time scale via a microstepper. A justification for ignoring the frequency drift is that frequent enough steering will remove it without significant impact.

In Section I, we present the notation associated with the Kalman filter. Section II briefly describes the LQG approach to finding the gains that produce minimum total cost. Section III shows what those costs are for every gain pair that leads to stable behavior. Section IV shows how the poles of the Z-transform are related to the time constants, stability, and performance variances. Section V relates the poles to the gains. Section VI shows how suboptimal state estimation degrades the steering. Section VII shows how to incorporate a time-lag in the application of measurements to steering decisions. Appendix I computes the Allan variances given the gains. Appendix II gives plots relating the gains, poles, and time constants. Appendix III solves the special case of frequency gain = 1 if there is suboptimal state estimation.

I. The basic equations

This section is a review of the Kalman filter [1-3], in order to define the notation in the presence of proportional steering in frequency. Following [5], we assume a system whose “true” and estimated states $x_{\text{true},k}$ and x_k are stable and defined by the difference between their phase and frequency with respect to a reference clock, $x_k = \begin{pmatrix} p_k \\ f_k \end{pmatrix}$. The steering goal is $p_k=f_k=0$. The discrete time series of state estimates, measured at times t_k , separated by intervals τ , is denoted x_k . The vector $x_{-,k}$ is the Kalman filter’s estimate of the true state function $x_{\text{true},k}$ at an instant just before the measurement at t_k , when its covariances are given in the matrix $P_{-,k}$. The measurement is assumed to be immediately utilized to create the state estimate x_k , and the frequency steering based upon that estimate is assumed to be immediately implemented.

The units are arbitrary in the sense that the “time coordinate” can be turns of phase, nanoseconds, or radians. The frequency and control (steering) terms have units of the time coordinate divided by the sampling interval τ , which is taken to be 1 in the figures that follow.

The measurement at time k yields a value m_k , and the details are:

$$m_k = Hx_{\text{true},k} + \nu_k \quad (1.1)$$

$$x_{\text{true},k} = \text{true value of } x_k \quad (\text{not its estimate}) \quad (1.2)$$

$$\Delta x_k = x_{\text{true},k} - (x_{-})_k \quad (\text{a 2x1 column vector}) \quad (1.3)$$

$$z_k = H\Delta x_k + \nu_k \quad (\text{termed the innovation, a scalar}) \quad (1.4)$$

$$H = \begin{pmatrix} 1 & 0 \end{pmatrix} = \text{measurement row vector} \quad (1.5)$$

$$\nu_k \text{ is the measurement noise, a scalar with autocovariance R} \quad (1.6)$$

Immediately after a measurement, the Kalman filter determines x_k

$$x_k = (x_{-})_k + K_g z_k \quad (1.7)$$

$$K_g = \text{Kalman Gain} = (P_-)_k H^T [H(P_-)_k H^T + R]^{-1} = \frac{1}{[R+(P_-)_{1,1}]} \begin{pmatrix} (P_-)_{1,1} \\ (P_-)_{2,1} \end{pmatrix} \quad (1.8)$$

$$P_k = \text{covariance of state estimate uncertainties (a } 2 \times 2 \text{ matrix)} \quad (1.9)$$

$$P_\infty = \text{limit of P after enough iterations to read steady-state} \quad (1.10)$$

The state estimate and its covariance just before and just after incorporating the measurement at estimation time k are as follows:

$$(x_-)_k = (\Phi - BG)x_{k-1} \quad (1.11)$$

$$x_k = (x_-)_k + K_g z_k = (x_-)_k + K_g (H \Delta x_k + v_k) \quad (1.12)$$

$$x_k = (1 - K_g H)(x_-)_k + K_g H x_{true,k} + K_g v_k \quad (1.13)$$

$$\Phi = \begin{pmatrix} 1 & \tau \\ 0 & 1 \end{pmatrix} = \begin{pmatrix} 1 & -\tau \\ 0 & 1 \end{pmatrix}^{-1} = \text{evolution matrix} \quad (1.14)$$

$$I = \begin{pmatrix} 1 & 0 \\ 0 & 1 \end{pmatrix} = \text{identity matrix} \quad (1.15)$$

$$B = \begin{pmatrix} \tau \\ 1 \end{pmatrix} = \Phi \begin{pmatrix} 0 \\ 1 \end{pmatrix} = \text{steer implementation vector propagated forward} \quad (1.16)$$

$$u_k = -G x_k = -G[(x_-)_k + K_g z_k] = \text{magnitude of steer} \quad (1.17)$$

$$G = (g_1 \ g_2) = \text{gain row vector} \quad (1.18)$$

(g_1 units are those of the phase divided by time, g_2 is dimensionless)

$$w_k = \text{process-noise vector before measurement k}; w_k w_k^T = Q \quad (1.19)$$

(In the examples we model the noise as a random walk in frequency, and in this case for $\tau=1$ the two components of w_k are the same.)

$$P_k = (I - K_g H)(P_-)_k = (I - K_g H)[\Phi P_{k-1} \Phi^T + Q] \quad (1.20)$$

$$P_k = \frac{R}{(R+(P_-)_{1,1})} \begin{pmatrix} (P_-)_{1,1} & (P_-)_{1,2} \\ (P_-)_{2,1} & (P_-)_{2,2} + \frac{1}{R} [(P_-)_{1,1}(P_-)_{2,2} + (P_-)_{1,2}(P_-)_{1,2}] \end{pmatrix} \quad (1.21)$$

$$(P_-)_{k+1} = \Phi P_k \Phi^T + Q = \Phi(I - K_g H)(P_-)_k \Phi^T + Q \quad (1.22)$$

$$(P_-)_{k+1} = \Phi(P_-)_k \Phi^T - \Phi(P_-)_k H^T [H(P_-)_k H^T + R]^{-1} H(P_-)_k \Phi^T + Q \quad (1.23)$$

$$(P_-)_{k+1} = \begin{pmatrix} (P_k)_{1,1} + (P_k)_{1,2} + (P_k)_{2,1} + (P_k)_{2,2} & (P_k)_{1,2} + (P_k)_{2,2} \\ (P_k)_{2,1} + (P_k)_{2,2} & (P_k)_{2,2} \end{pmatrix} + Q \quad (1.24)$$

II. Optimization via Linear Quadratic Gaussian (LQG) approach

The LQG approach finds the value of the gain vector G that minimizes the total cost, defined as a linear combination of the phase, frequency, and frequency-steer variances [1-5]; the coefficients of those variances are the component costs. Of the three cost parameters, only two are independent parameters, since an overall scaling does not affect the minima. As described in the references, and following the notation already presented, one first solves a Riccati equation for K_o and then the optimal gain vector G is determined as follows:

$$K_o = \Phi^T K_o \Phi + W_Q - \Phi^T K_o B (B^T K_o B + K_W B)^{-1} B^T K_o \Phi \quad (2.1)$$

$$G = (B^T K_o B + K_o W_R)^{-1} B^T K_o \Phi \quad (2.2)$$

where the costs for time/freq stability are W_Q , and the cost for control is W_R . $W_Q(1,1)$ has dimension $1/\tau^2$, while $W_Q(2,2)$ and W_R are dimensionless. A reason to minimize the control variance is because the controlled clock is usually more stable than the reference for small τ , and excessive steering will destabilize short-term performance. Using Matlab, one can find the desired gains with a function call: $[K_o, G, 0] = \text{dlqr}(\Phi, B, W_Q, W_R, 0)$. As a consequence of the Separation Theorem, these expressions are independent of the noise variances R and Q, although they do depend on the sampling interval.

The solutions are summarized in figures 2.1-2.2, which show the phase and frequency gains as a function of the costs, scaled so that the control cost is 1. As expected, the gains indicated are consistent with the minima in the figures that follow.

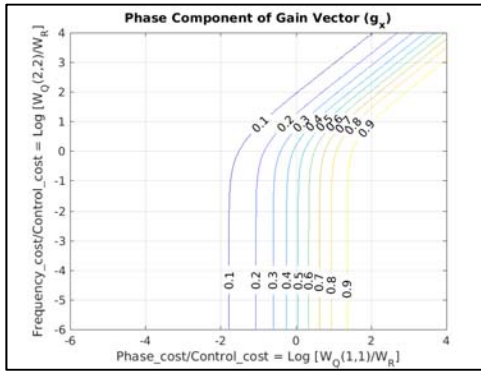


Figure 2.1. Optimal phase gain as function of cost ratios.

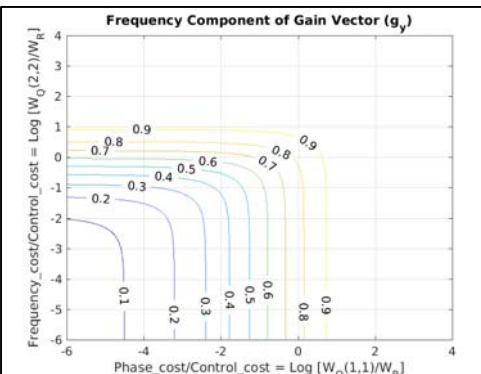


Figure 2.2 Optimal frequency gain as function of cost ratios

III. The expected variances of the phase, frequency, and frequency steers as functions of the gain vector, in steady-state.

It is possible to compute the expected variances of the phase, frequency, and steers for any set of gains that yield finite steady-state results in the long term. We show in equation 4.38 that this stability standard requires only that $4-\tau g_1 - 2g_2 > 0$, although all gains > 1 lead to oscillatory behavior.

Using the Kalman formalism, the steady state covariance P_∞ and associated Kalman Gain $K_{g,\infty}$ can be found by replacing both $(P_-)_k$ and $(P_-)_{k+1}$ in equation 1.8 with P_- . With Matlab, one would call $[P_- \infty, L, F] = dare(\Phi^T, H^T, Q, R)$, where L are the eigenvalues, and $F = (HP_\infty H^T + R)^{-1} HP_\infty$. The estimated steady-state covariance is

$$P_\infty = (I - K_{g,\infty} H) P_- = (I - \begin{pmatrix} K_1 & 0 \\ K_2 & 0 \end{pmatrix}) P_- = \begin{pmatrix} 1 - K_1 & 0 \\ -K_2 & 1 \end{pmatrix} P_- \quad (3.1)$$

Equation 1.23 can be used to find the associated Kalman Gain, $K_{g,\infty}$. After enough iterations to reach steady-state, the state evolution equation can be written, with all the gain-dependent terms absorbed into A , where

$$A = (\Phi - BG) = \begin{pmatrix} 1 & \tau \\ 0 & 1 \end{pmatrix} - \begin{pmatrix} \tau \\ 1 \end{pmatrix} (g_1 \quad g_2) = \begin{pmatrix} 1 - g_1 \tau & \tau(1 - g_2) \\ -g_1 & 1 - g_2 \end{pmatrix} \quad (3.2)$$

$$(x_-)_{k+1} = (\Phi - BG)x_k = Ax_k = A[(x_-)_k + K_{g,\infty}(H \Delta x_k + v_k)] \quad (3.3)$$

$$(x_-)_{k+1} = A(x_-)_k + AK_{g,\infty}H \Delta x_k + AK_{g,\infty}v_k \quad (3.4)$$

Dropping the subscripts of $K_{g,\infty}$,

$$(x_-)_k = Ax_{k-1}; \quad <(x_-)_k(x_-)_k^T> = \Sigma_{x_-} = A\Sigma_x A^T \quad (3.5)$$

$$<(x_-)_k(x)_k^T> = A <(x)_{k-1}(x)_{k-1}^T> = A\Sigma_x \quad (3.6)$$

$$\Delta x_k = x_{true,k} - (x_-)_k = \Phi x_{true,k-1} + w_k - BGx_{k-1} - (\Phi - BG)x_{k-1} \quad (3.7)$$

$$\Delta x_k = \Phi(x_{true,k-1} - x_{k-1}) + w_k \quad (3.8)$$

$$\Delta x_k = \Phi(x_{true,k-1} - (x_-)_{k-1} - KH\Delta x_{k-1} - Kv_{k-1}) + w_k \quad (3.9)$$

$$\Delta x_k = \Phi(1 - KH)\Delta x_{k-1} - \Phi Kv_{k-1} + w_k \quad (3.10)$$

$$\Sigma_{\Delta x} = <\Delta x_k \Delta x_k^T> = \Phi(1 - KH)\Sigma_{\Delta x}[\Phi(1 - KH)]^T + \Phi K R K^T \Phi^T + Q \quad (3.11)$$

This is a Lyapunov equation, in Matlab: $\Sigma_{\Delta x} = dlyap(\Phi(1 - KH), \Phi K R K^T \Phi^T + Q)$

$$\Sigma_x = <x_k x_k^T> = <[(x_-)_k + K(H \Delta x_k + v_k)][(x_-)_k + K(H \Delta x_k + v_k)]^T> \quad (3.12)$$

Since the noise parameter v_k and the prediction error Δx_k are uncorrelated with each other and $(x_-)_k$ (though not x_k):

$$\Sigma_x = \Sigma_{x_-} + KH\Sigma_{\Delta x}(KH)^T + KRK^T \quad (3.13)$$

Using equation 3.5, we derive a Lyapunov equation for Σ_x :

$$\Sigma_x = A\Sigma_x A^T + KH\Sigma_{\Delta x}(KH)^T + KRK^T \quad (3.14)$$

The variance of the control, u , is

$$\langle u^2 \rangle = \langle G x_k x_k^T G^T \rangle = G \Sigma_x G^T \quad (3.15)$$

The expressions derived are for the best available state estimates. A secondary observer measuring the state with negligible noise, and with knowledge of the steers being implemented, would find lower variances as follows:

$$\Sigma_{true,x} = \langle x_{true,k} x_{true,k}^T \rangle \quad (3.16)$$

$$\text{Using 3.8, } \Sigma_{\Delta x} = \langle (\Phi(x_{true,k-1} - x_{k-1}) + w_k)(\Phi(x_{true,k-1} - x_{k-1}) + w_k)^T \rangle \quad (3.17)$$

$$\Sigma_{\Delta x} = \langle \Phi x_{true,k-1} - \Phi x_{k-1} + w_k \rangle (\Phi x_{true,k-1} - \Phi x_{k-1} + w_k)^T \quad (3.18)$$

$$\Sigma_{\Delta x} = \Phi \Sigma_{true,x} \Phi^T - \Phi \langle x_{true,k-1} x_{k-1}^T \rangle \Phi^T - \Phi \langle x_{k-1} x_{true,k-1}^T \rangle \Phi^T + \Phi \Sigma_x \Phi^T + Q \quad (3.19)$$

$$\text{But } \langle x_{true,k-1} x_{k-1}^T \rangle = \Sigma_{true,x} \quad (3.20)$$

$$\Phi \Sigma_{true,x} \Phi^T = \Phi \Sigma_x \Phi^T - \Sigma_{\Delta x} + Q \quad ; \quad \Sigma_{true,x} = \Sigma_x + \Phi^{-1}(Q - \Sigma_{\Delta x})\Phi^{-1,T} \quad (3.21)$$

Since the secondary observer's variances differ from the Kalman-derived ones by expressions that do not depend on the gains (which would have entered through the matrix A), their minima with respect to the gains are unchanged.

The derivation of the expected Allan deviations (and Hadamard variances) is a straightforward extension of the formulas developed in this section, and provided in Appendix I. We now present some illustrative numerical results and figures.

Table 1 shows the phase, frequency, and control RMS for three sets of gains and several possible values for measurement and process noise. The gains are those that would minimize the phase variance, with a gain vector $G=(1,1)$, or almost minimize the frequency variance with $G=(0.01,1)$ - a phase gain of zero was avoided because it would result in unbounded phase variations.

sqrt(R)	sqrt(Q)	Phase RMS	Freq RMS	Cntrl RMS	Phase RMS	Freq RMS	Cntrl RMS
Phase_gain=1 Freq_gain=1					Phase_gain=.01 Freq_gain=1		
0.100	0.0001	0.05	0.04	0.07	0.32	0.01	0.01
0.100	0.0100	0.16	0.18	0.30	1.13	0.10	0.10
0.100	1.0000	1.02	1.42	2.26	7.22	1.00	1.01
0.316	0.0001	0.08	1.51	0.12	0.58	0.01	0.01
0.316	0.0016	0.16	0.16	0.26	1.15	0.04	0.04
0.316	1.0000	1.14	1.51	2.43	8.10	1.00	1.01
1.000	0.0001	0.14	0.14	0.21	1.09	0.01	0.01
1.000	0.0100	0.45	0.46	0.71	3.24	0.10	0.11
1.000	1.0000	1.60	1.88	3.05	11.35	1.01	1.02
1.000	10.0000	3.61	4.80	7.68	25.62	3.17	3.20
1.000	1000.0000	31.69	44.76	70.80	224.61	31.70	31.94
3.162	0.0001	0.25	0.25	0.36	2.08	0.02	0.02
3.162	0.0100	0.80	0.80	1.20	5.85	0.11	0.12
3.162	1.0000	2.62	2.80	4.46	18.55	1.02	1.03

Table 1. Minimum attainable phase, frequency, and control RMS for an uncontrolled clock, as a function of the measurement and process noise

Figures 3.1-3.6 show the RMS as a function of gains for two different sets of process and measurement noise; they are normalized so that their minima are 1.

The plot titles have a “Ph” for phase, an “F” for Frequency, or a “C” for control. The phase and frequency gains (pg and fg) at the minimum value are also indicated, and the value of the pre-normalization minimum (min) is indicated at the end. To avoid unbounded behavior the minimum gains plotted were 0.01.

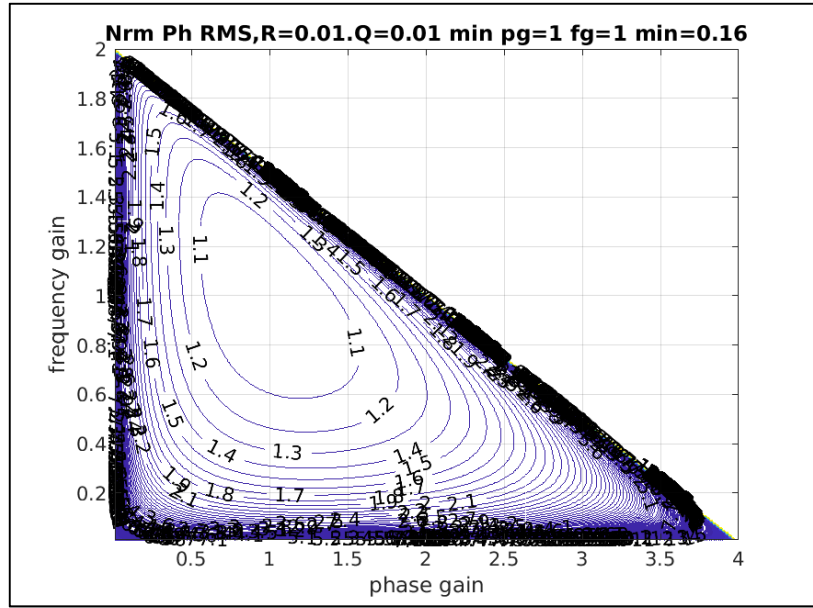


Figure 3.1 Normalized phase RMS as function of gains, $R=0.1$, $Q=0.01$

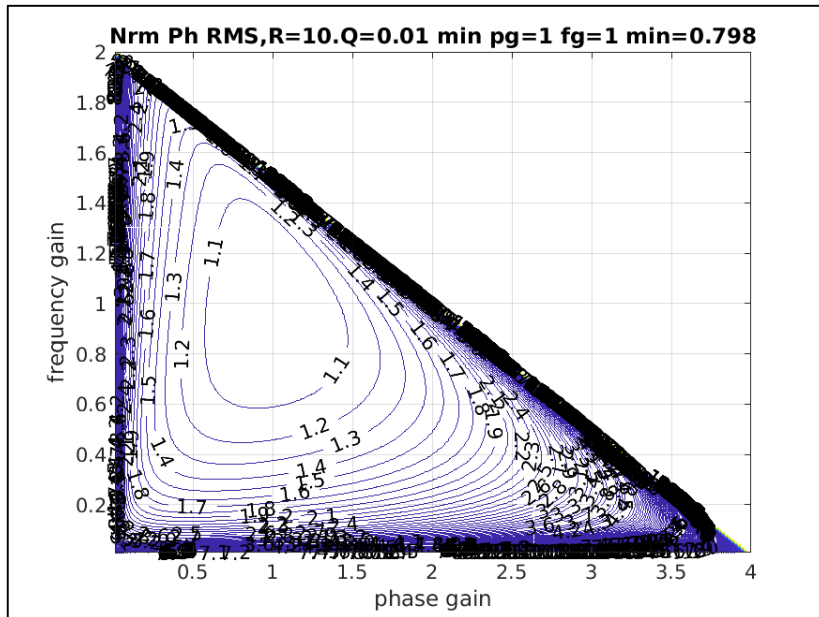


Figure 3.2 Normalized phase RMS as function of gains, $R=10$, $Q=0.01$

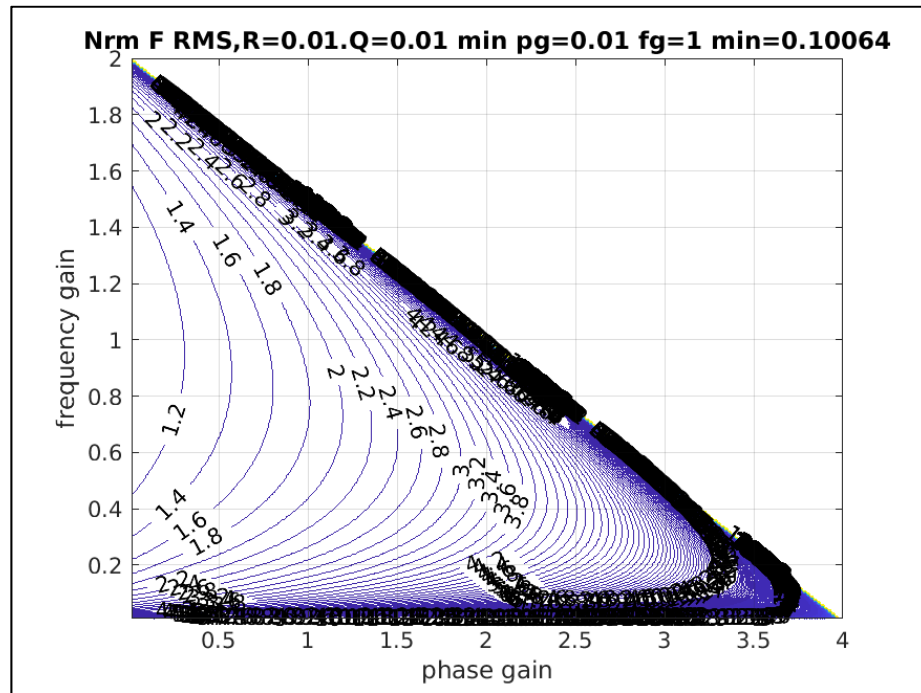


Figure 3.3 Normalized frequency RMS as function of gains, $R=0.01$, $Q=0.01$

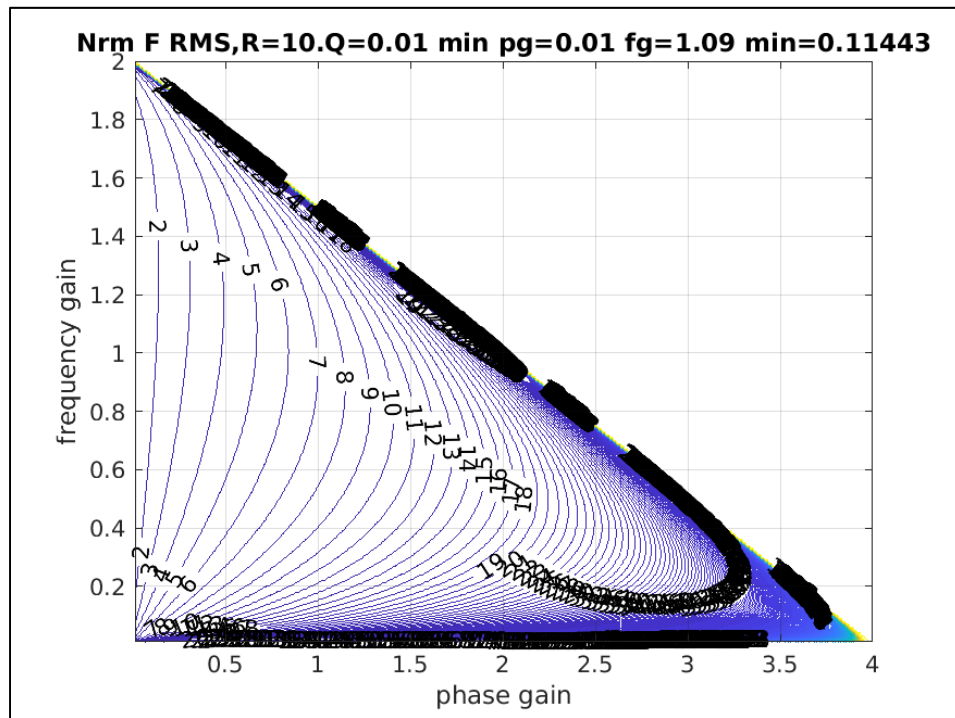


Figure 3.4 Normalized frequency RMS as function of gains, $R=10$, $Q=0.01$

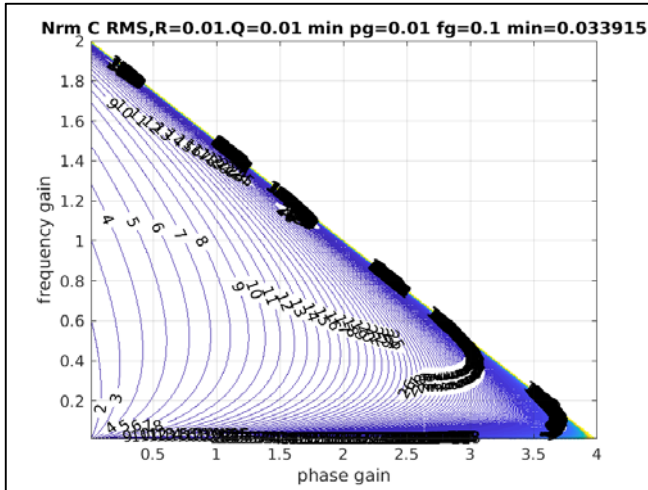


Figure 3.5 Normalized control RMS as function of gains, R=0.01, Q=0.01

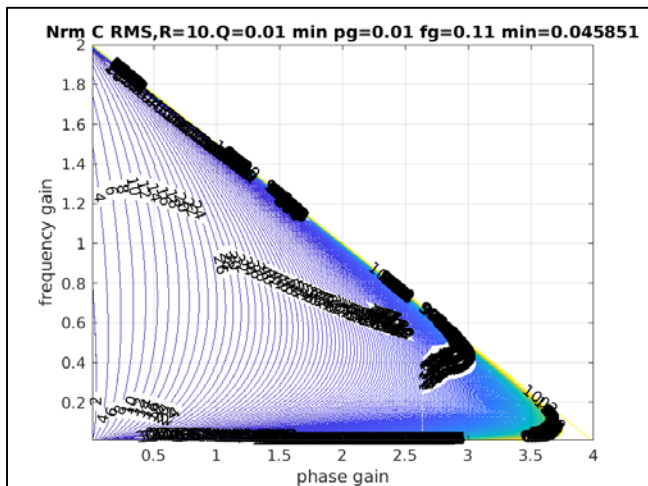


Figure 3.6 Normalized control RMS as function of gains, R=10, Q=0.01

Figures 3.7-3.9 show the simulated behavior when a clock whose behavior is an integrated random walk is steered either with minimal gains or gains that would minimize the frequency or phase of the controlled clock after being optimally estimated with a Kalman filter. Process and measurement noises were 1. So as to avoid large deviations, gains that should have been 0 for optimality were set to 0.01. For example, the optimal reduction of frequency RMS requires a phase gain of 0, which would result in unbounded phase deviations.

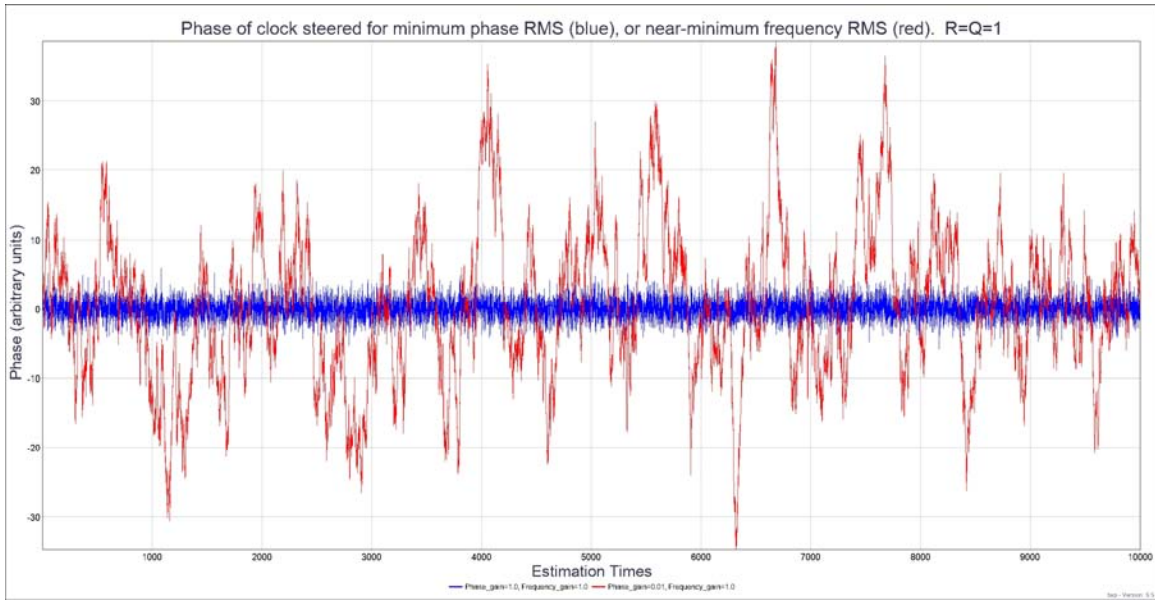


Figure 3.7. Phase behavior of clock of controlled to minimize phase RMS (blue, RMS=1.6) or frequency RMS (red, RMS=11).

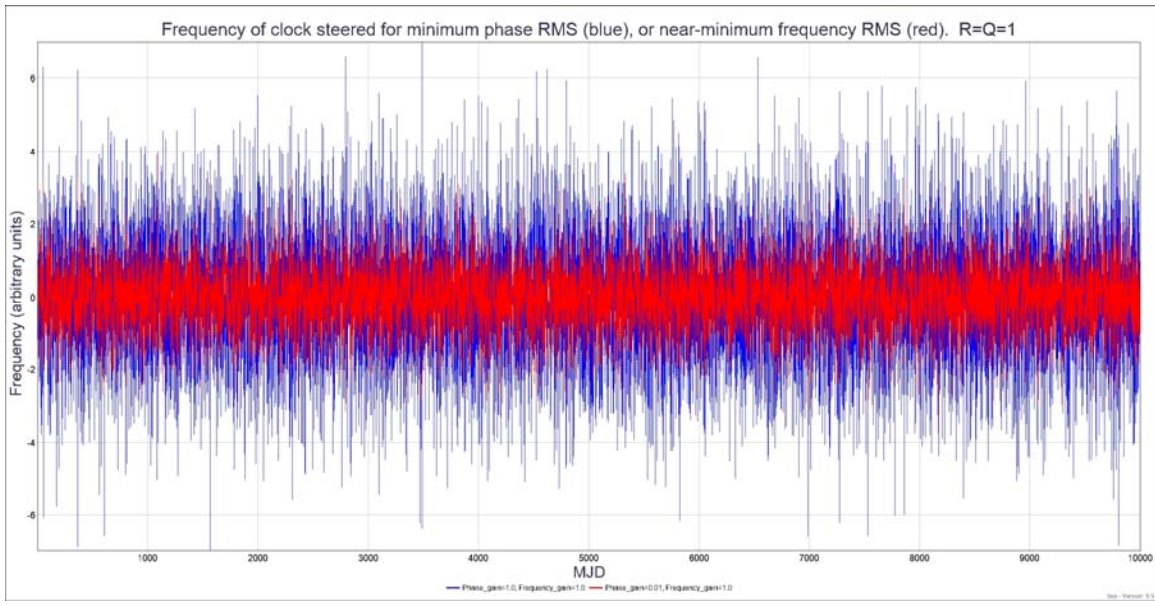


Figure 3.8. Frequency behavior of clock controlled to minimize phase RMS (blue, RMS=1.9) or frequency RMS (red, RMS=1.0).

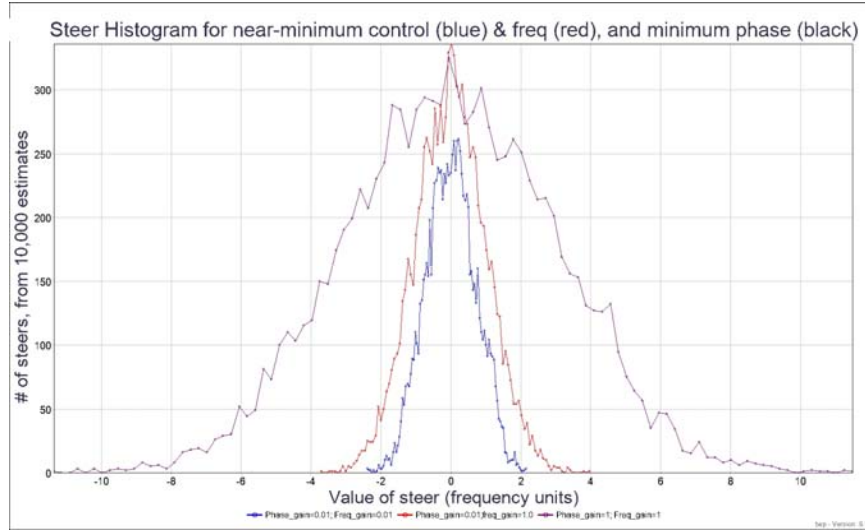


Figure 3.9. Histograms of steers when set to minimize phase, frequency, or controls. To avoid unbounded situations, a gain that would be exactly 0 is set to 0.01.

Figures 3.10-3.15 display normalized total cost curves for three different values of the cost function, and two different measurement noise cases. As required by the Separation Theorem, the minima are independent of the assumed R and Q values, although the width and shape of the contours are different; in our 2-state formulation they depend only the ratio of the measurement noise to the process noise. Plot titles are as in Figure 3.1, except that “pc” and “fc” indicate the phase and frequency costs.

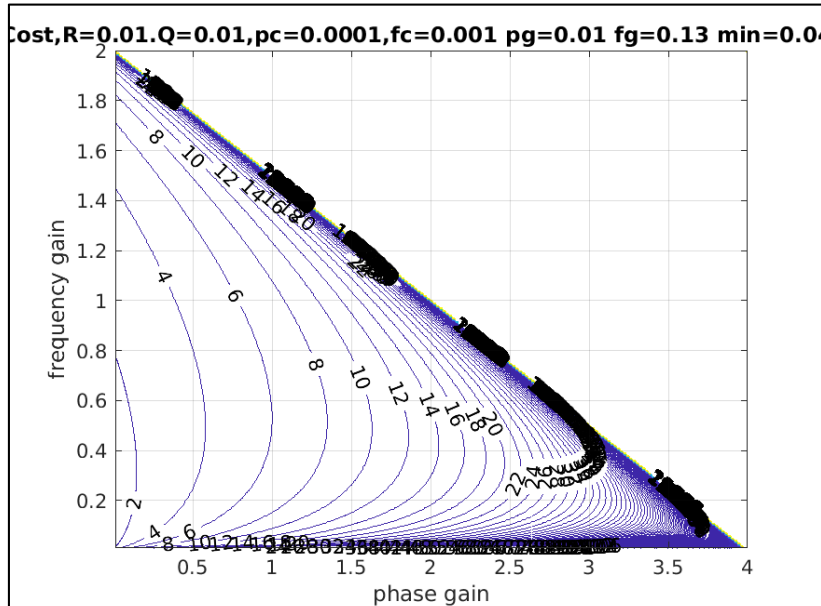


Figure 3.10. Normalized total costs for measurement noise $R=0.01$ and process noise $Q=0.01$, when phase, frequency, and control variance costs are $.0001, .001$, and 1 respectively.

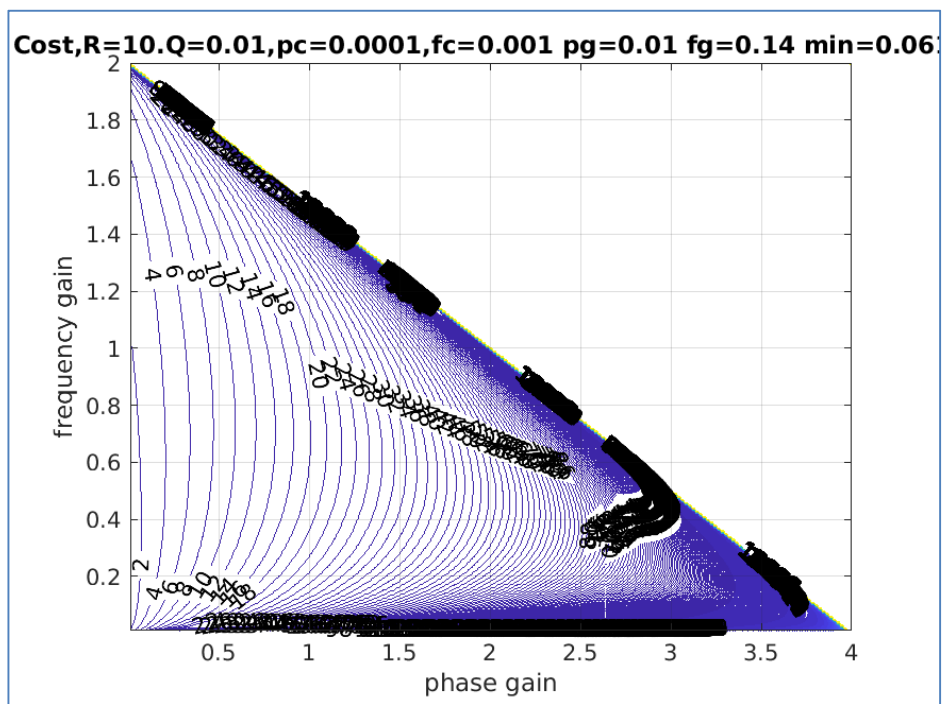


Figure 3.11. Normalized total costs for measurement noise $R=10$ and process noise $Q=0.01$, when phase, frequency, and control variance costs are .0001,.001, and 1 respectively.

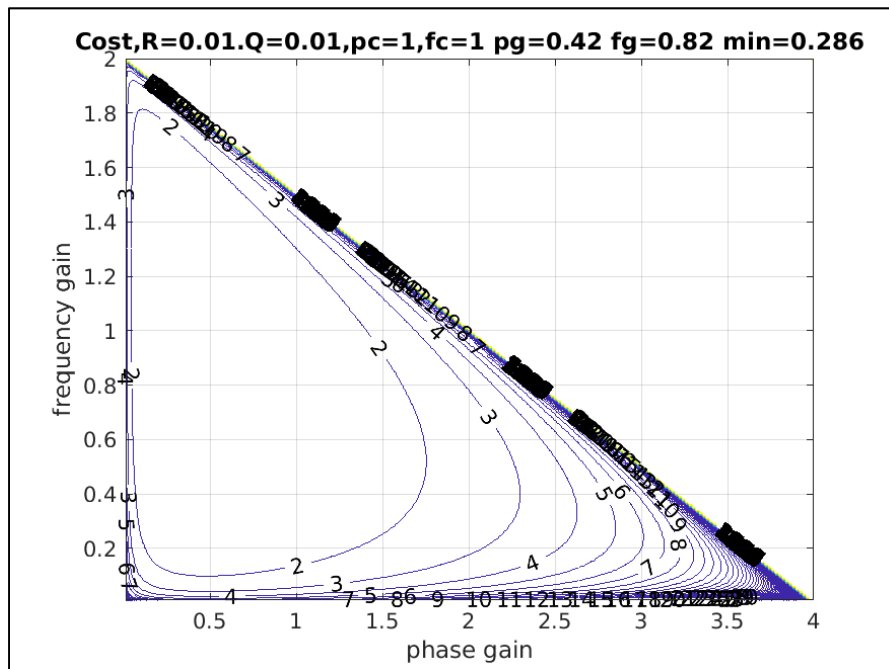


Figure 3.12. Normalized total costs for measurement noise $R=0.01$ and process noise $Q=0.01$, when phase, frequency, and control variance costs are all 1.

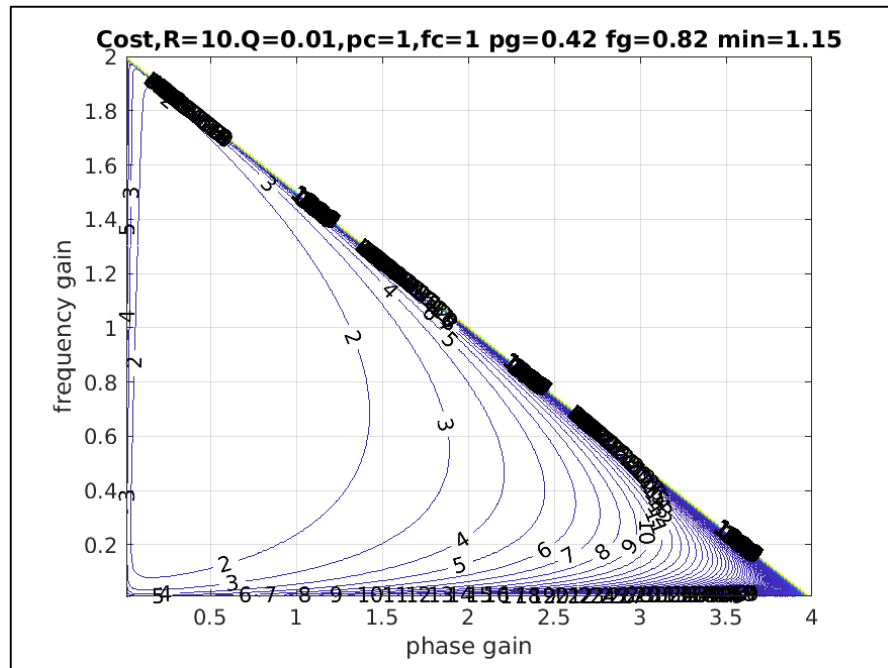


Figure 3.13. Normalized total costs for measurement noise $R=10$ and process noise $Q=0.01$, when phase, frequency, and control variance costs are all 1.

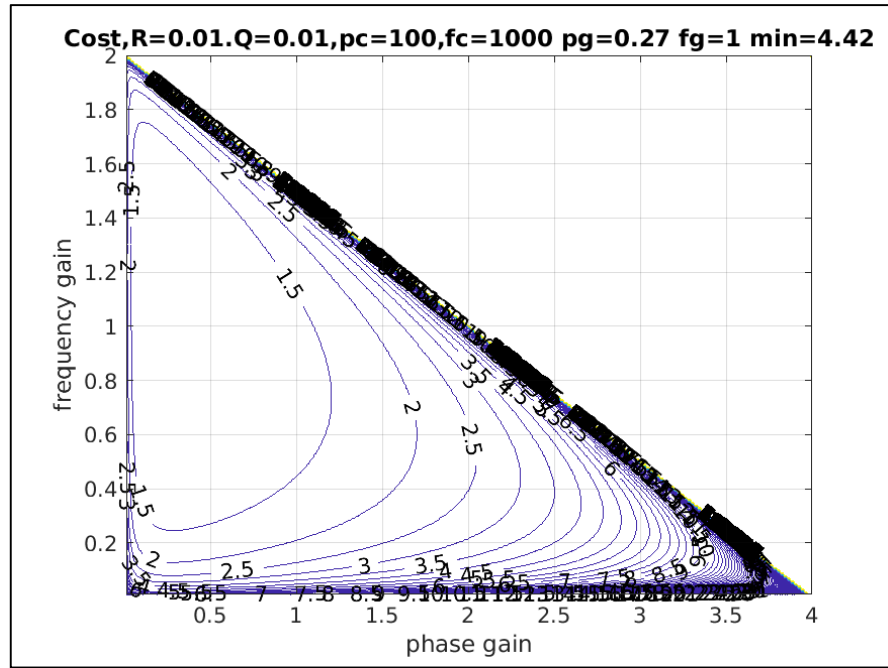


Figure 3.14. Normalized total costs for measurement noise $R=0.01$ and process noise $Q=0.01$, when phase, frequency, and control variance costs are 100, 1000, and 1 respectively.

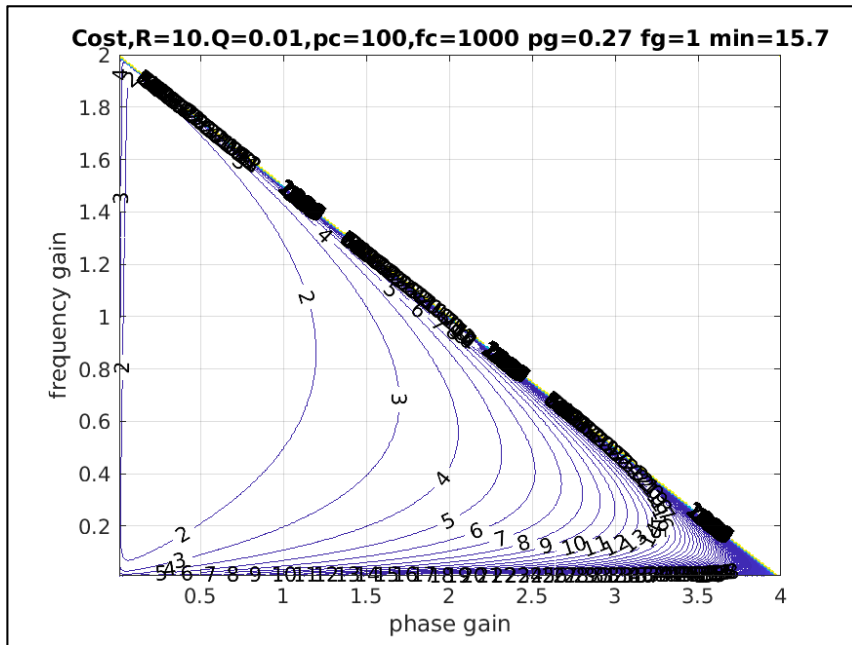


Figure 3.15. Normalized total costs for measurement noise $R=10$ and process noise $Q=0.01$, when phase, frequency, and control variance costs are 100, 1000, and 1 respectively.

IV. The time constants, as determined by the poles in the Z-transform

In order to develop this approach, we explicitly work with the phase and frequency components of the state vector (p_k and f_k), and note that f_k is $(p_k - p_{k-1})/\tau$.

The Z-transform of a time series p_k can be written:

$$X(z) = \sum_{k=0}^{k=\infty} p_k z^{-k} \quad (4.1)$$

Here x is a scalar (the phase), and for exponential decay with time constant T ,

$$p_k = p_0 e^{-k\tau/T} \quad (4.2)$$

$$\frac{X(z)}{p_0} = \sum_{k=0}^{k=\infty} e^{-k\tau/T} z^{-k} = \sum_{k=0}^{k=\infty} (ze^{\tau/T})^{-k} = 1/(1 - 1/(ze^{\tau/T})) = z/(z - e^{-\tau/T}) \quad (4.3)$$

Therefore the pole of the z-transform is $e^{-\tau/T}$. To be stable, we require

$$|e^{-\tau/T}| < 1 \quad (4.4)$$

Using equation 1.14:

$$p_k = (2 - \tau g_1 - g_2)p_{k-1} - (1 - g_2)p_{k-2} + n_k \quad (4.6)$$

where the frequency $y_{k-1} = (p_{k-1} - p_{k-2})/\tau$ and n_k is the combined effects of the uncorrelated process noise and optimally-filtered measurement noises from $k=0$.

Taking the Z-transform of both sides:

$$X(z) = (2 - \tau g_1 - g_2) \sum_{k=0}^{k=\infty} p z^{-k} - (1 - g_2) \sum_{k=0}^{k=\infty} p_{k-2} z^{-k} + \sum_{k=0}^{k=\infty} n_k z^{-k} \quad (4.7)$$

$$X(z) = (2 - \tau g_1 - g_2)z^{-1}X(z) - (1 - g_2)z^{-2}X(z) + extras \quad (4.8)$$

$$extras = (2 - \tau g_1 - g_2)p_{-1} - (1 - g_2)(p_{-2} + p_{-1}) + \sum_{k=0}^{k=\infty} n_k z^{-k} \quad (4.9)$$

$$X(z) = (extras)/[1 - (2 - \tau g_1 - g_2)z^{-1} + (1 - g_2)z^{-2}] \quad (4.10)$$

$$X(z) = (extras)z^2/[z^2 + (\tau g_1 + g_2 - 2)z + (1 - g_2)] \quad (4.11)$$

The “extras” incorporate the initial conditions and the noise, while the poles and their associated time constants T_{pole} are given by

$$e^{-\tau/T_{pole}} = z_{pole} = (2 - \tau g_1 - g_2)/2 \pm \sqrt{\left(\frac{(2-\tau g_1 - g_2)}{2}\right)^2 - (1 - g_2)} \quad (4.12)$$

We note that equation 4.12 can also be derived from the eigenvalue equation $Ax_k = e^{-\tau/T_{pole}}x_k$, and this is developed in Section VII.

$$\text{The solution is critically damped } (T=T_c) \text{ if: } \left(\frac{(2-\tau g_1 - g_2)}{2}\right)^2 = (1 - g_2) \quad (4.13)$$

$$\text{or } 2 - \tau g_1 - g_2 = \pm 2\sqrt{(1 - g_2)} \quad (4.14)$$

$$\tau g_1 = 2 - g_2 \pm 2\sqrt{(1 - g_2)} = (1 \pm \sqrt{1 - g_2})^2 \quad (4.15)$$

$$\pm \sqrt{\tau g_1} = 1 \pm \sqrt{1 - g_2} \quad (4.16)$$

$$(1 \pm \sqrt{\tau g_1})^2 = 1 \pm 2\sqrt{\tau g_1} + \tau g_1 = 1 - g_2 \quad (4.17)$$

$$\text{Since the gains must be } >= 0, \quad g_2 = 2\sqrt{\tau g_1} - \tau g_1 \quad (4.18)$$

Because the discriminant in 4.12 is now zero, the equation for T_c becomes [5,6]:

$$e^{-\tau/T_c} = \frac{(2-\tau g_1 - g_2)}{2} = 1 - \sqrt{\tau g_1} = \sqrt{(1 - g_2)} \quad (4.19)$$

$$T_c = \frac{-\tau}{\ln(1 - \sqrt{\tau g_1})} = -2/\ln(1 - g_2) \quad (4.20)$$

$$g_1 = \tau^{-1}(1 - e^{-\tau/T})^2 \quad (4.21)$$

$$g_2 = 1 - e^{-2\tau/T} \quad (4.22)$$

If the solution is not critically damped, the discriminant in equation 4.12 is not zero:

$$disc^2 = \left(\frac{(2-\tau g_1 - g_2)}{2}\right)^2 - (1 - g_2) = \frac{(\tau g_1)^2}{4} + \frac{(g_2)^2}{4} + \tau g_1 g_2 / 2 - \tau g_1 \quad (4.32)$$

If the discriminant is negative there will be two oscillation frequencies. Expressing the pole components as $re^{i\theta} = e^{-\tau/T}e^{i\theta} = e^{-\tau/T}e^{2\pi i f_{osc}\tau}$, where f_{osc} is the frequency of the oscillations, the decay constant T is given by the magnitude of 4.12:

$$e^{-\tau/T} = \sqrt{(1 - g_2)} \quad (4.33)$$

$$\text{and the frequency is } f_{osc} = \frac{1}{2\pi\tau} \tan\left[\frac{4(1-g_2)}{(2-\tau g_1 - g_2)^2} - 1\right] \quad (4.34)$$

If the discriminant is positive, there are two time constants and the magnitude of their associated terms will depend upon the details of the disturbances that excite them. If one of the poles is negative, there is oscillatory behavior with frequency $f_{osc} = \frac{1}{2\tau}$, since $e^{i\theta} = -1$

Poles near the origin of the unit circle have a smaller value of $\exp(-\tau/T)$ and therefore a faster response and a smaller decay time T. A pole on the origin of the unit circle has an “infinitely fast” response. Poles near the unit circle have a slower response (large time constant T), consistent with the gains being low. Poles outside the unit circle are unstable. Lower frequency gains yield oscillatory behavior while larger gains have two associated time constants.

Figure 4.1 shows how the positive, negative, mixed, and imaginary pole configurations are a function of phase and frequency gain. The unit circle is mapped onto the diagonal line segment which marks the boundary of stability. The term “critically damped” is generally applied only when the gains are <1, however we apply it to all cases wherein the discriminant is zero, even if the pole is negative and therefore oscillatory.

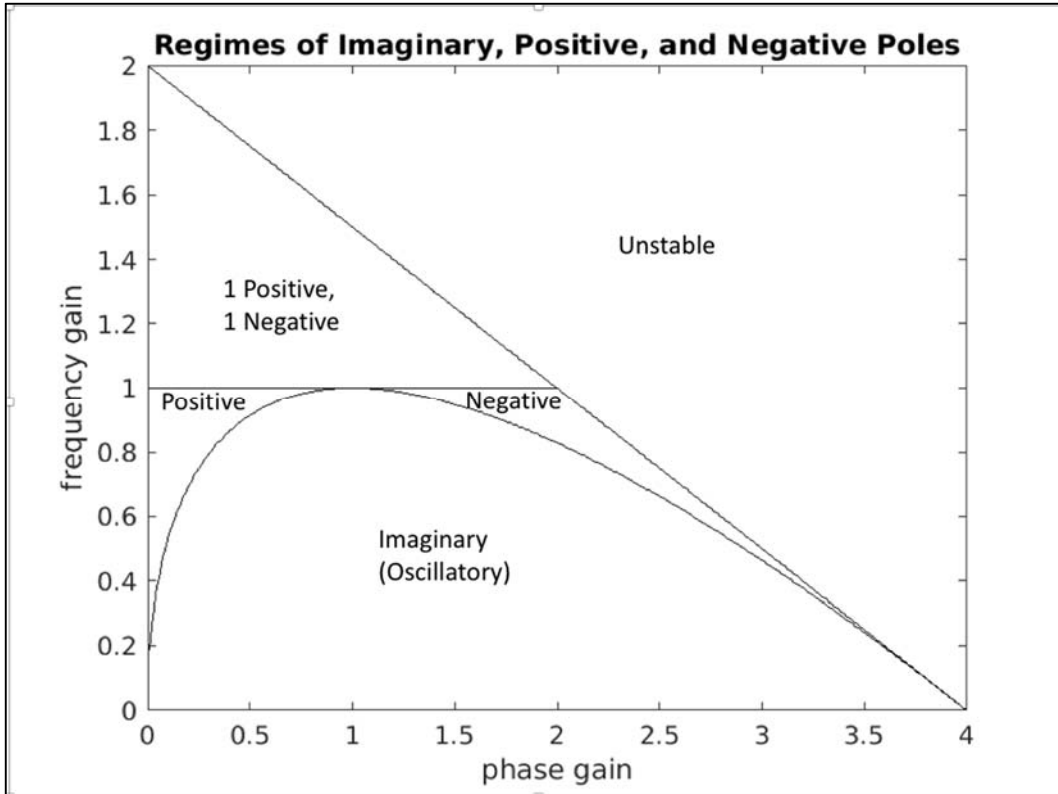


Figure 4.1. Areas of stable, oscillatory, or unstable behavior as function of gains. Non-oscillatory, stable behavior exists only when both poles are positive.

Equation 4.12 can be used to explicitly demonstrate that the unit circle delineates the region of stability, defined as where a finite impulse yields a finite response. The largest absolute value of z_{pole} occurs when the two terms being summed on the right-hand side have the same sign. If the first term is negative and the discriminant is positive, the equation at the point of instability reduces to

$$z_{pole} = -1 = \frac{(2-\tau g_1 - g_2)}{2} - \sqrt{\left\{ \left(\frac{(2-\tau g_1 - g_2)}{2} \right)^2 - (1 - g_2) \right\}} \quad (4.35)$$

$$-2 + \frac{(\tau g_1 + g_2)}{2} = \sqrt{\left\{ -1 + g_2 + \left(\frac{(2-\tau g_1 - g_2)}{2} \right)^2 \right\}} = \sqrt{\left\{ \frac{(\tau g_1)^2}{4} + \frac{(g_2)^2}{4} - \tau g_1 + \tau g_1 g_2 / 2 \right\}} \quad (4.36)$$

Squaring both sides,

$$4 - 2(\tau g_1 + g_2) + \frac{(\tau g_1)^2}{4} + \frac{(g_2)^2}{4} + \frac{\tau g_1 g_2}{2} = \frac{(\tau g_1)^2}{4} + \frac{(g_2)^2}{4} - \tau g_1 + \frac{\tau g_1 g_2}{2} \quad (4.37)$$

$$4 - \tau g_1 - 2g_2 = 0 \quad (4.38)$$

If the first term is positive and the discriminant is positive,

$$z_{pole} = 1 = \frac{(2-\tau g_1 - g_2)}{2} + \sqrt{\left\{ \frac{(\tau g_1)^2}{4} + \frac{(g_2)^2}{4} - \tau g_1 + \frac{\tau g_1 g_2}{2} \right\}} \quad (4.39)$$

$$\frac{(\tau g_1)^2}{4} + \frac{(g_2)^2}{4} + \frac{\tau g_1 g_2}{2} = \frac{(\tau g_1)^2}{4} + \frac{(g_2)^2}{4} - \tau g_1 + \frac{\tau g_1 g_2}{2} \text{ and the boundary is at } g_1 = 0.$$

If the discriminant is negative, equation 4.40 applies and the boundary is at $g_2 = 0$.

Figure 4.2 shows an example in which the controlled clock undergoes a large step and is brought back to the reference with the phase gain is set to 0.2 and a variety of frequency gains (0.1 to 1.0). The smoothest response is for the critical gain, near 0.694, which is shown with circles.

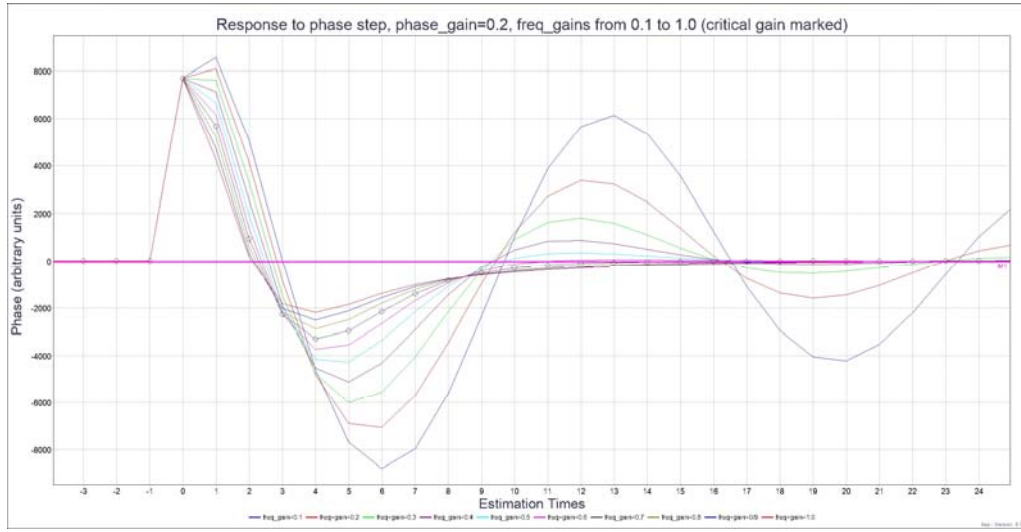


Figure 4.2. Response to a step in the controlled clock for a phase gain of 0.2 and a variety of frequency gains. The critical gain is near 0.7 and shown with circles. Oscillatory behavior characterizes the cases with lower frequency gains, while two time constants are at work for frequency gains above critical.

Using the formulas of section III, it is possible to plot the interplay between the critical gains and their associated time constants (Figure 4.1), as well as the RMS associated with them (Figures 4.3-4.5). These illustrate the fact that the performance is more sensitive to frequency gain than control gain, and that right steering degrades frequency performance.

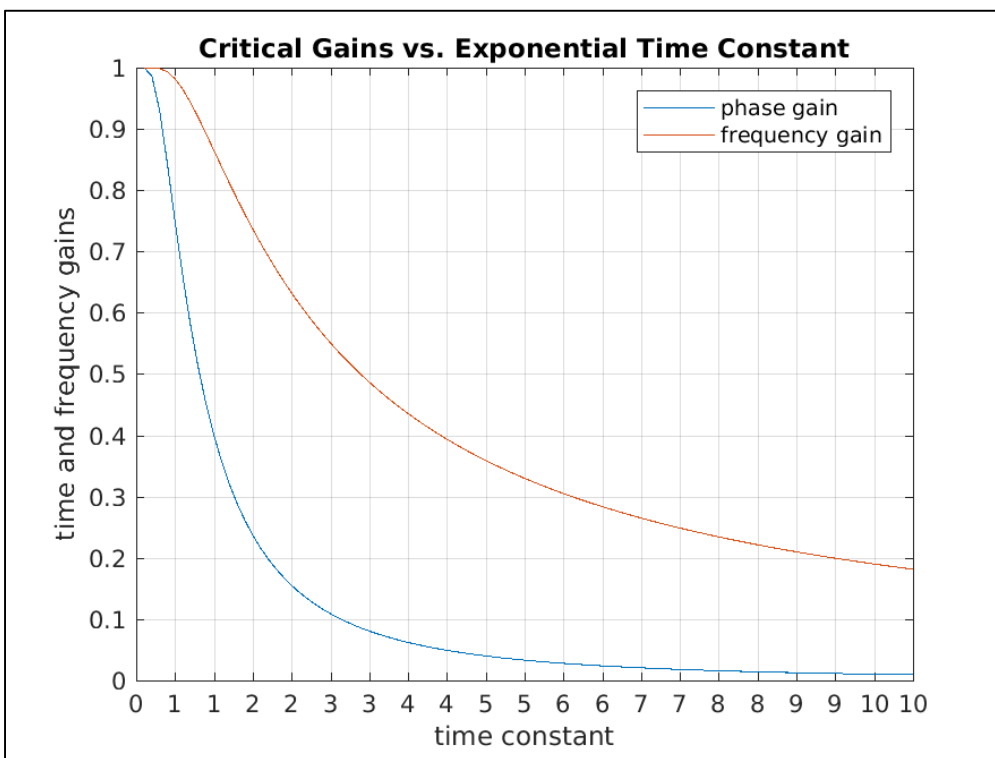


Figure 4.3. Critical phase and frequency gains as a function of time constant, in units of the measurement interval. The frequency gain is always higher.

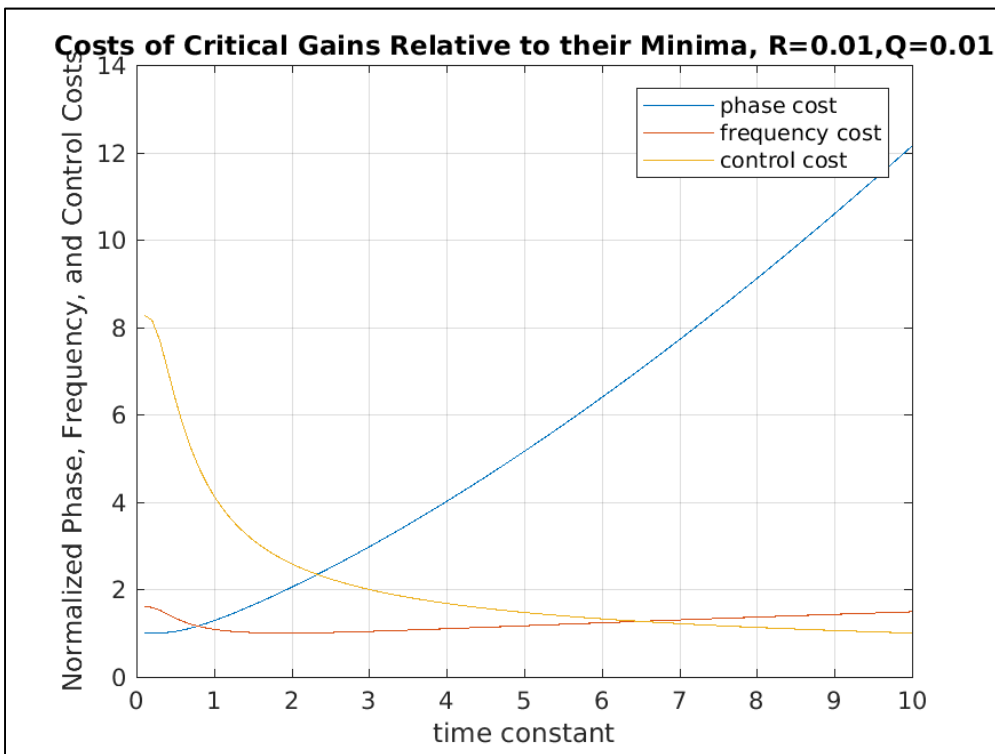


Figure 4.4. Normalized Phase, Frequency, and Control RMS as function of time constant, for critical gains, measurement noise $R=0.01$, and process noise $Q=0.01$.

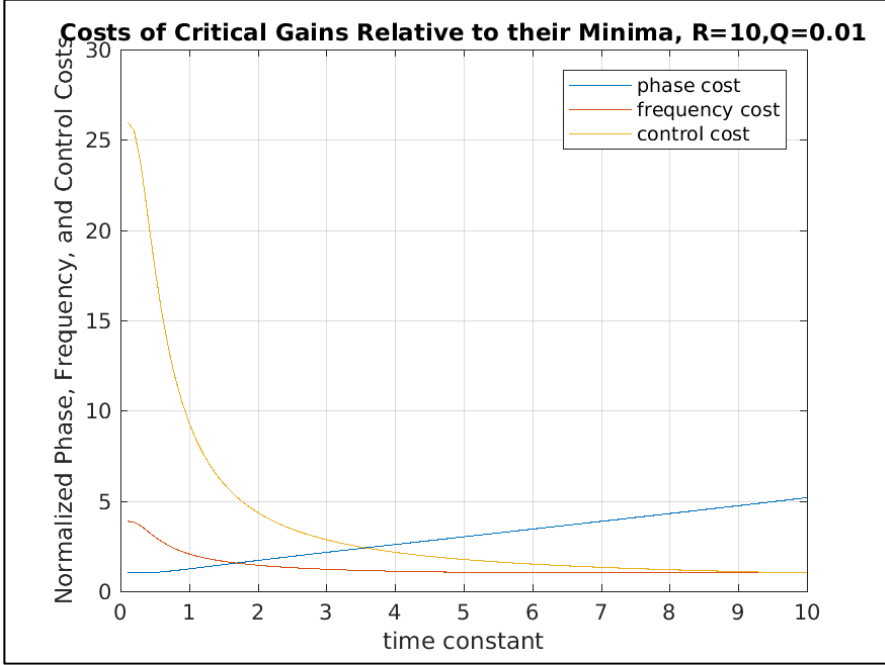


Figure 4.5. Normalized Phase, Frequency, and Control RMS as function of time constant, for critical gains, measurement noise $R=10$, and process noise $Q=0.01$.

V. Finding the gains, given the poles.

Assume you have two real poles, $-1 < P_i < 1$, $\tau g_1 < 4$, and $g_2 < 2$, and:

$$\text{Let } b = (\tau g_1 + g_2 - 2); \text{disc} = (\tau g_1 + g_2 - 2)^2 - 4(1 - g_2) > 0 \quad (5.1, 5.2)$$

$$\text{Then } P_1 = \frac{-b}{2} + \frac{1}{2}\sqrt{\text{disc}} \quad ; \quad P_2 = \frac{-b}{2} - \frac{1}{2}\sqrt{\text{disc}} \quad (5.3, 5.4)$$

$$b = -(P_1 + P_2) \quad ; \quad \text{disc} = (P_1 - P_2)^2 = P_1^2 - 2P_1P_2 + P_2^2 \quad (5.5, 5.6)$$

$$\text{disc} - b^2 = -4P_1P_2 = -4(1 - g_2) \quad ; \quad P_1P_2 = (1 - g_2) \quad (5.7)$$

$$g_2 = 1 - P_1P_2 \quad ; \quad \tau g_1 = 2 + b - g_2 = 1 - P_1 - P_2 + P_1P_2 \quad (5.8, 5.9)$$

Assume the poles are imaginary. They are complex conjugates of each other, $\tau g_1 < 2$, $g_2 < 1$, and:

$$P_{real} = \text{Re}(P_1) = \text{Re}(P_2) = \frac{-b}{2} \quad ; \quad P_{real} = \frac{2-\tau g_1-g_2}{2} \quad (5.10)$$

$$P_{imag} = \text{Im}(P_i) = \frac{\sqrt{-\text{disc}}}{2} = \sqrt{1 - g_2 - \frac{b^2}{4}} = \sqrt{1 - g_2 - \frac{(2-\tau g_1-g_2)^2}{4}} \quad (5.11)$$

$$P_{real}^2 + P_{imag}^2 = 1 - g_2 \quad ; \quad g_2 = 1 - P_{real}^2 - P_{imag}^2 \quad (5.12)$$

$$\tau g_1 = 2 + b - g_2 = 2 - 2P_{real} - g_2 = 1 - P_{real}^2 + P_{imag}^2 \quad (5.13)$$

The mapping between the gains, the pole locations within the unit circle, the decay times, and oscillatory frequencies is explored in Appendix II.

VI. Suboptimal estimates

The Separation Theorem does not imply that the optimal gains derived by LQG are optimal if the state itself is not optimally estimated. An obvious example would be a state measured with a system that always returns the same value no matter what the state is; in that case setting both gains to zero may be the best no matter what performance is desired. A more common error is to assume that the measurements of the state are noiseless, and that the frequency is exactly found through differencing the last two measurements. Using equation 1.11, the following equation shows that this is equivalent to setting the Kalman gain $K = \begin{pmatrix} 1 \\ 1 \end{pmatrix}$:

$$\begin{pmatrix} p_k \\ f_k \end{pmatrix} = \begin{pmatrix} 2p_{k-1} - p_{k-2} \\ p_{k-1} - p_{k-2} \end{pmatrix} + K(p_{true,k} - 2p_{k-1} + p_{k-2} + v_k) = \begin{pmatrix} p_{true,k} + v_k \\ p_{true,k} - p_{k-1} + v_k \end{pmatrix} \quad (6.1)$$

Following the formalism already developed in Section III, one can replace the steady state Kalman gain with the suboptimal gain K and follow all the equations up to and including 3.12, as in:

$$\Sigma_x = \langle x_k x_k^T \rangle = \langle [(x_-)_k + K(H \Delta x_k + v_k)][(x_-)_k + K(H \Delta x_k + v_k)]^T \rangle \quad (6.2)$$

However, in the analog to equation 3.13 some new terms appear because the predicted state is no longer uncorrelated with the prediction error Δx_k .

$$\Sigma_x = \Sigma_{x_-} + \Sigma_{x_\Delta x} (KH)^T + KH \langle \Delta x_k \Delta x_k^T \rangle (KH)^T + KH \Sigma_{x_\Delta x}^T + KRK^T \quad (6.3)$$

, where $\Sigma_{x_\Delta x} = \langle (x_-)_k \Delta x_k^T \rangle$ and as before $\Sigma_{\Delta x} = \langle \Delta x_k \Delta x_k^T \rangle$.

The second and fourth terms in 6.3 are not zero because, while the optimal prediction is just as likely to differ positively as negatively from the true value no matter what its sign is, our suboptimal estimate's difference with the true value is more likely to have the same sign. Using equation 3.5:

$$\Sigma_x = A \Sigma_x A^T + \Sigma_{x_\Delta x} (KH)^T + KH \Sigma_{\Delta x} (KH)^T + KH \Sigma_{x_\Delta x}^T + KRK^T \quad (6.4)$$

Using 3.10, $\Sigma_{x_\Delta x} = \langle (x_-)_k [\Phi(1 - KH) \Delta x_{k-1} - \Phi K v_{k-1} + w_k]^T \rangle \quad (6.5)$

$$\Sigma_{x_\Delta x} = \langle (x_-)_k \Delta x_{k-1}^T \rangle [\Phi(1 - KH)]^T - AKRK^T \Phi^T \quad (6.6)$$

$$\Sigma_{x_\Delta x} = A \langle x_{k-1} \Delta x_{k-1}^T \rangle [\Phi(1 - KH)]^T - AKRK^T \Phi^T \quad (6.7)$$

$$\langle x_{k-1} \Delta x_{k-1}^T \rangle = \langle [(x_{-})_{k-1} + K(H \Delta x_{k-1} + v_{k-1})] \Delta x_{k-1}^T \rangle \quad (6.8)$$

$$\langle x_{k-1} \Delta x_{k-1}^T \rangle = \langle x_{-,k-1} \Delta x_{k-1}^T \rangle + KH \Sigma_{\Delta x} \quad (6.9)$$

$$\Sigma_{x_{\Delta x}} = A[\langle x_{-,k-1} \Delta x_{k-1}^T \rangle + KH \Sigma_{\Delta x}] [\Phi(1 - KH)]^T - AKRK^T \Phi^T \quad (6.10)$$

$$\Sigma_{x_{\Delta x}} = A\Sigma_{x_{\Delta x}} [\Phi(1 - KH)]^T + AKH \Sigma_{\Delta x} [\Phi(1 - KH)]^T - AKRK^T \Phi^T \quad (6.11)$$

$$A^{-1} \Sigma_{x_{\Delta x}} = \Sigma_{x_{\Delta x}} [\Phi(1 - KH)]^T + KH \Sigma_{\Delta x} [\Phi(1 - KH)]^T - KRK^T \Phi^T \quad (6.12)$$

Equation 6.12 is a Sylvester's equation, solvable in Matlab as

$$\Sigma_{x_{\Delta x}} = \text{sylvester}(A^{-1}, -[\Phi(1 - KH)]^T, KH \Sigma_{\Delta x} [\Phi(1 - KH)]^T - KRK^T \Phi^T) \quad (6.13)$$

Using 3.5, one can now solve equation 6.4 as a Lyapunov equation:

$$\Sigma_x = \text{dlyap}(A, KH \Sigma_{\Delta x} (KH)^T + KRK^T + C + C^T); \quad C = \Sigma_{x_{\Delta x}} (KH)^T \quad (6.14)$$

$$\text{The control effort can be found as in 3.15: } \langle u^2 \rangle = G \Sigma_x G^T \quad (6.15)$$

Unfortunately, the above formalism is invalid for the special case where $g_2=1$, because the matrix $A = \begin{pmatrix} 1-g_1 & 0 \\ -g_1 & 0 \end{pmatrix}$ is singular and cannot be inverted for 6.12. One could interpolate over those particular points, but Appendix III shows how to solve exactly for them.

To compute the statistics of the optimal estimates, with the steering still based on the suboptimal value, we define $\Delta K = K - K_{\text{opt}}$ and $(x_{\text{opt},k})$ as what x_k would be if it had been optimally estimated at each interval, with that optimal estimate not being used for the steering.

$$x_{\text{opt},k} = x_k - \Delta K H \Delta x_k - \Delta K v_k \quad (6.16)$$

$$\Sigma_{\text{opt},k} = \Sigma_k + \Delta K H \Sigma_{\Delta x} (\Delta K H)^T + \Delta K R (\Delta K)^T - \Sigma_{x_{\Delta k}} (\Delta K H)^T - \Delta K H \Sigma_{x_{\Delta k}}^T \quad (6.17)$$

$$\text{where } \Sigma_{x_{\Delta x}} = \langle x_k \Delta x_k^T \rangle = \langle x_{-,k} \Delta x_k^T \rangle + KH \langle \Delta x_k \Delta x_k^T \rangle = \Sigma_{x_{\Delta x}} + KH \Sigma_{\Delta x} \quad (6.18)$$

The ratios shown in figures 6.1-6.6 are the RMS for the suboptimal case divided by the optimal RMS, for two different cases of process and measurement noise. In our 2-state formulation, the fractional degradation depends on the ratio of the measurement noise to the process noise. As would be expected, the figures show that the consequences of the noiseless approximation become more serious as the measurement noise R increases. For $R=0.1$ and $Q=1$, all ratios are within 5% of optimal.

In some cases, the ratios are less than unity for low gains, particularly for the phase RMS. This is partly because the low gains in effect average over the noise much as an optimal state estimator would filter them out, and also because the mis-estimation of the frequency and phase would be

correlated for every point, which leads to larger steers and so the gains are effectively larger – thus reducing the phase and frequency offsets faster.

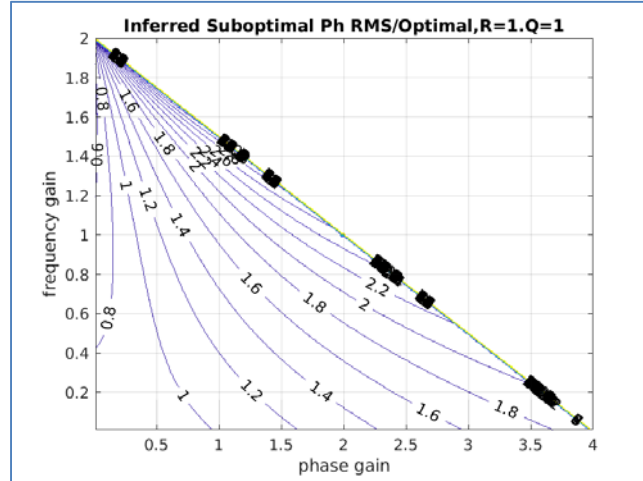


Figure 6.1. Ratio of phase RMS to optimal, when state suboptimally estimated and $R=1$ and $Q=1$

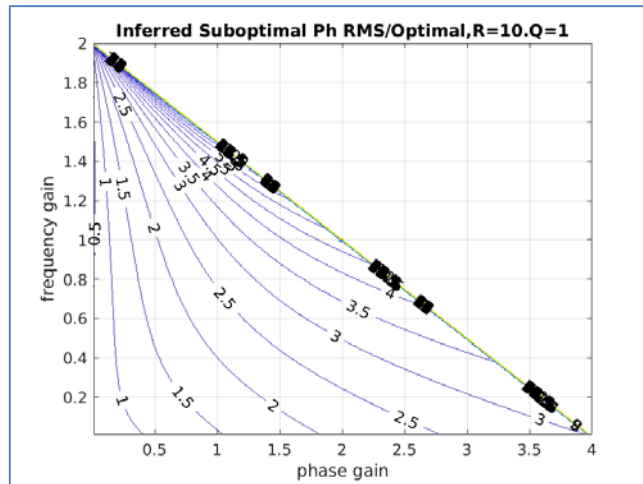


Figure 6.2. Ratio of phase RMS to optimal, when state suboptimally estimated and $R=10$ and $Q=1$

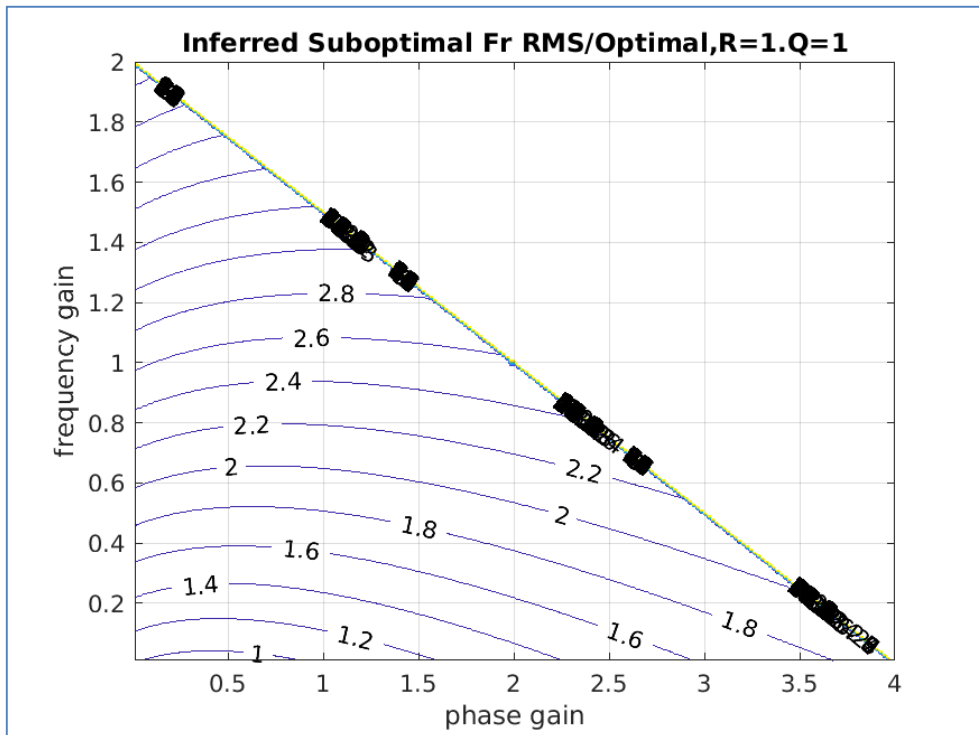


Figure 6.3. Ratio of frequency RMS to optimal, when state suboptimally estimated and $R=1$ and $Q=1$

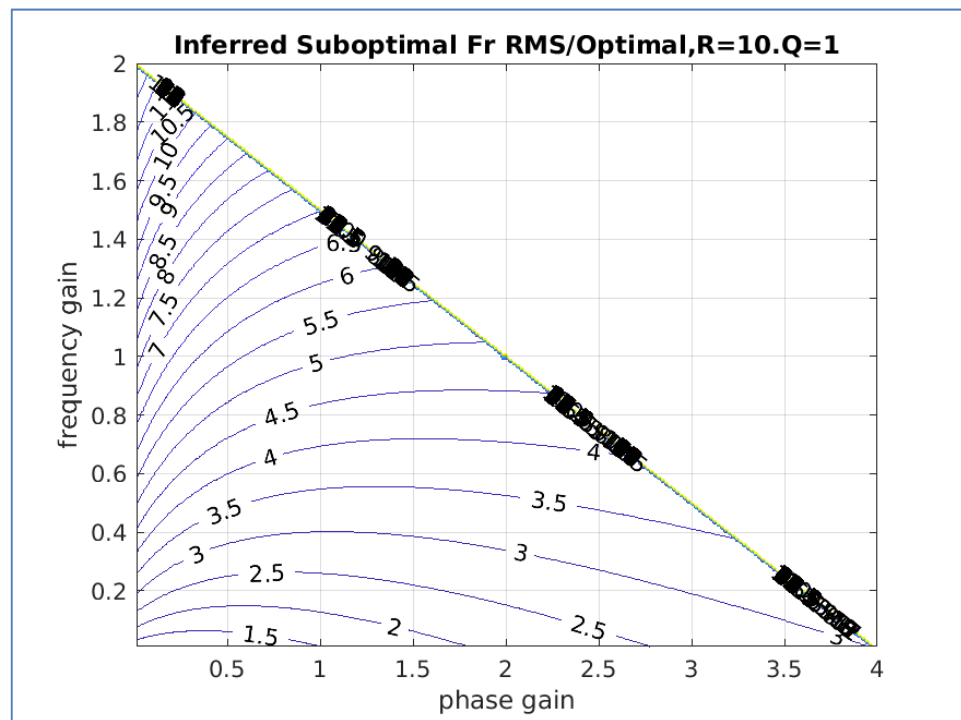


Figure 6.4. Ratio of frequency RMS to optimal, when state suboptimally estimated and $R=10$ and $Q=1$

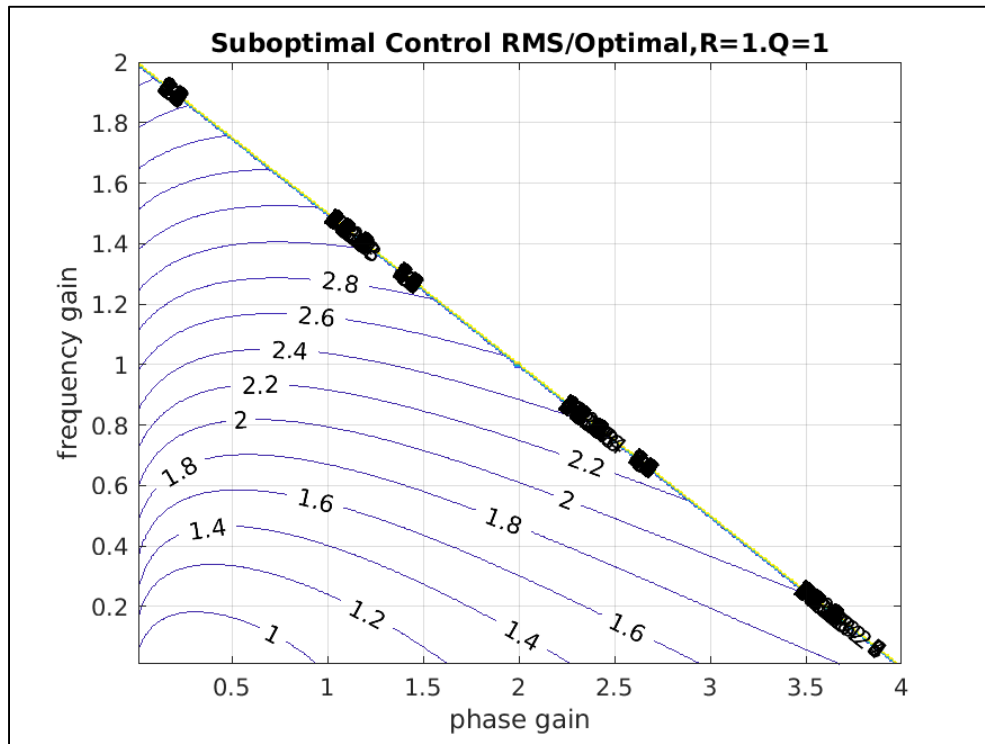


Figure 6.5. Ratio of control RMS to optimal, when state suboptimally estimated and R=1 and Q=1

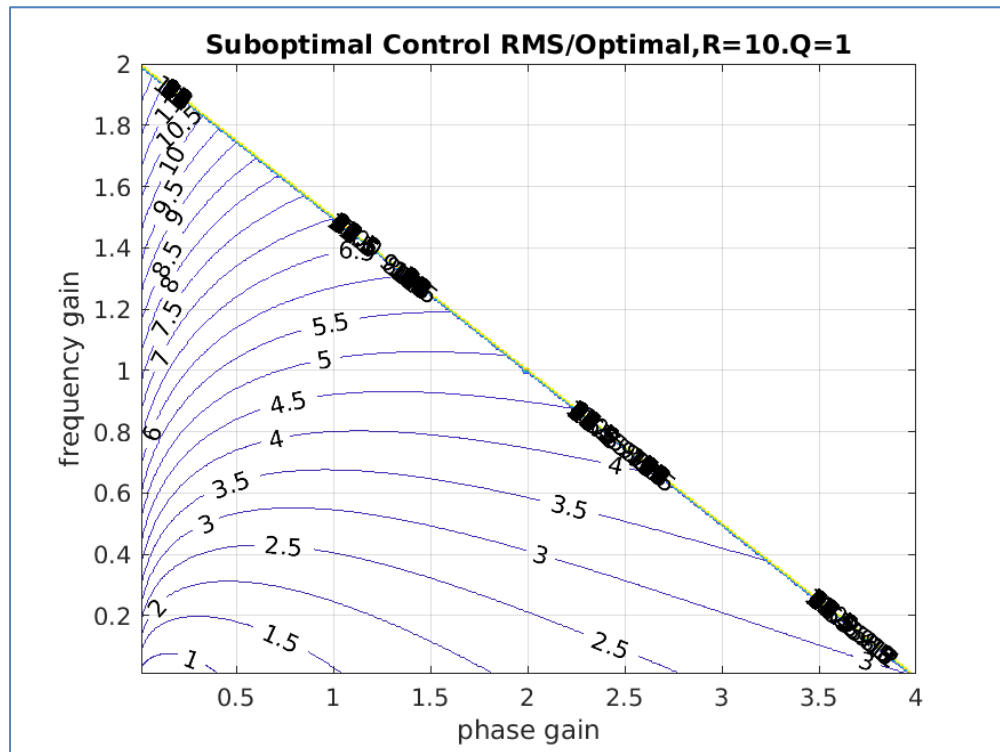


Figure 6.6. Ratio of control RMS to optimal, when state suboptimally estimated and R=10 and Q=1

Figures 6.7 and 6.8 show simulations of phase and frequency stability requests for optimal and suboptimal estimates, assumed to be noiseless.

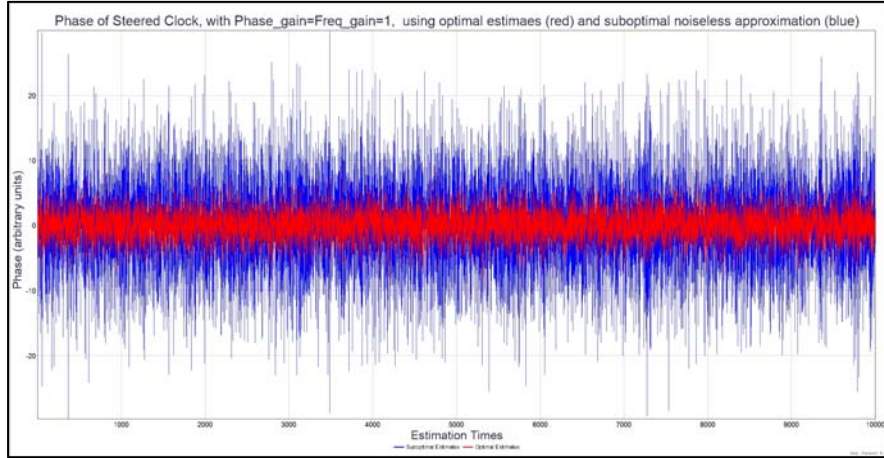


Figure 6.7 Simulated phase of controlled clock when state estimates are optimal (red, $R=10$, $Q=1$), or suboptimal because measurements are assumed to be noiseless (blue, $R=0$, $Q=1$). The RMS phases are 7.7 and 2.6.

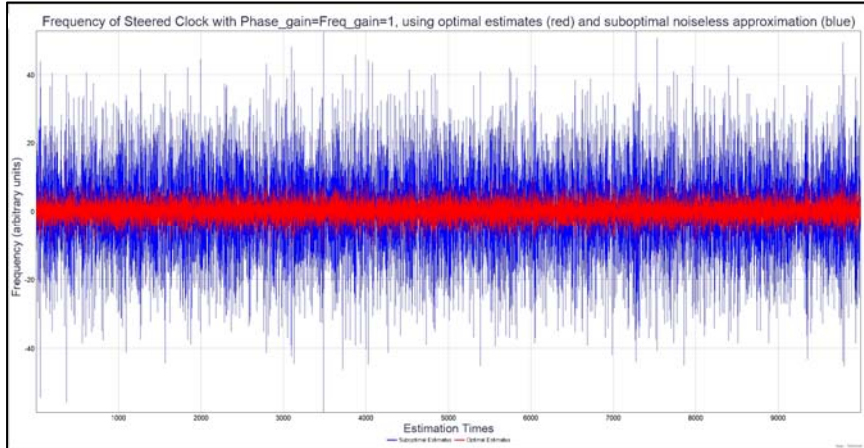


Figure 6.8. Simlated frequency of controlled clock when state estimates are optimal (red, $R=10$, $Q=1$), or suboptimal because measurements are assumed to be noiseless (blue, $R=0$, $Q=1$). The RMS frequencies are 14 and 2.7.

VII. Steering when there is an information lag.

In steering a master clock to UTC, the information needed to steer comes in 30-day batches, approximately 10 days late. A similar situation exists for Rapid UTC (UTCr), which is computed in 7-day batches, arriving about 3 days late. We approximate this by setting τ equal to the batch size, and assuming a steer is implemented only after a fractional lag $\lambda < 1$. Any available measurements between times k and $k-1$ can be used to estimate x_k , so long as they take into account the steers $s_{k+\lambda}$ applied within that interval. The prediction of the state at the time the

information is received (and implemented) is based upon propagating the last known state forward to the time the information is delivered (with Φ_λ) and the steers can be denoted $s_{k+\lambda}$.

$$\Phi_\lambda = \begin{pmatrix} 1 & \lambda\tau \\ 0 & 1 \end{pmatrix}; \quad B_\lambda = \begin{pmatrix} \tau(1-\lambda) \\ 1 \end{pmatrix}; \quad s_{k+\lambda} = G\Phi_\lambda x_k \quad (7.1)$$

The first part of equation 3.3 becomes:

$$(x_-)_{k+1} = (\Phi - B_\lambda s_{k+\lambda})x_k = (\Phi - B_\lambda G\Phi_\lambda)x_k \quad (7.2)$$

And then the rest of Section 3's mathematics follow directly if one replaces A by A_λ , where

$$A_\lambda = (\Phi - B_\lambda G\Phi_\lambda) = \begin{pmatrix} 1 - (1-\lambda)\tau g_1 & \tau - (1-\lambda)\tau(\lambda\tau g_1 + g_2) \\ -g_1 & 1 - \lambda\tau g_1 - g_2 \end{pmatrix} \quad (7.3)$$

$$\text{and the control variance is } \langle s_{k+\lambda} s_{k+\lambda}^T \rangle = G\Phi_\lambda \Sigma_k (G\Phi_\lambda)^T \quad (7.4)$$

In order to study the associated time constants, it is possible to develop the eigenvalue approach, which is complementary to the Z-transform method provided in Section 4. Ignoring measurement and process noise, and denoting the eigenvalues as E:

$$x_{k+1} = A_\lambda x_k = Ex_k \quad (7.5)$$

$$\text{The eigenvalues satisfy } |A_\lambda - \begin{pmatrix} E & 0 \\ 0 & E \end{pmatrix}| = 0 \quad (7.6)$$

The determinant equation is

$$0 = (1 - (1-\lambda)\tau g_1 - E)(1 - \lambda\tau g_1 - g_2 - E) + g_1(\tau - (1-\lambda)\tau(\lambda\tau g_1 + g_2)) \quad (7.7)$$

$$0 = E^2 + (-2 + g_2 + \tau g_1)E + (1 - g_2) \quad (7.8)$$

The solution to this is identical to (4.12), with the eigenvalues $E = e^{-\tau/T_{pole}}$. Since this expression does not depend on the lag λ , the time constants would be the same function of the gains as derived previously.

Figures 7.1-7.3 show the ratio of phase, frequency, and control RMS, as a function of gain, to their values when there is no lag. The ratios are still closer to unity for clocks that have lower process noise. While reducing the rather modest degradations due to the phase lag are one reason for the large improvements observed when laboratories steer to UTC using UTCr, the principle reason is that the weekly spacing of the UTCr deliveries entails considerably less process noise between estimates than is associated with the monthly spacing of the UTC deliveries via the Circular T.

Note that the phase costs for non-zero lags are always larger than for zero lag when the gains are less than 1, but can be less otherwise. This can be understood as follows: if the phase and frequency

offsets have the same (positive) sign, the steer will be more negative due to the phase increase over the lag, thus tending to counteract the frequency more and lowering the contribution of the next measured point to the phase variance. It is equally likely that only the frequency offset is negative and then the computed steer would be less, tending to increase the contribution of the next measured point to the variance. The symmetry is broken because the variance depends on the square of the offsets, and it is therefore more sensitive to changes in the larger values that happen when phase and frequency offsets have the same sign. Even so, the reduction in variance is only with regards to the measurement points; inserting the steers in between measurements adds instabilities within the intervals between measurements.

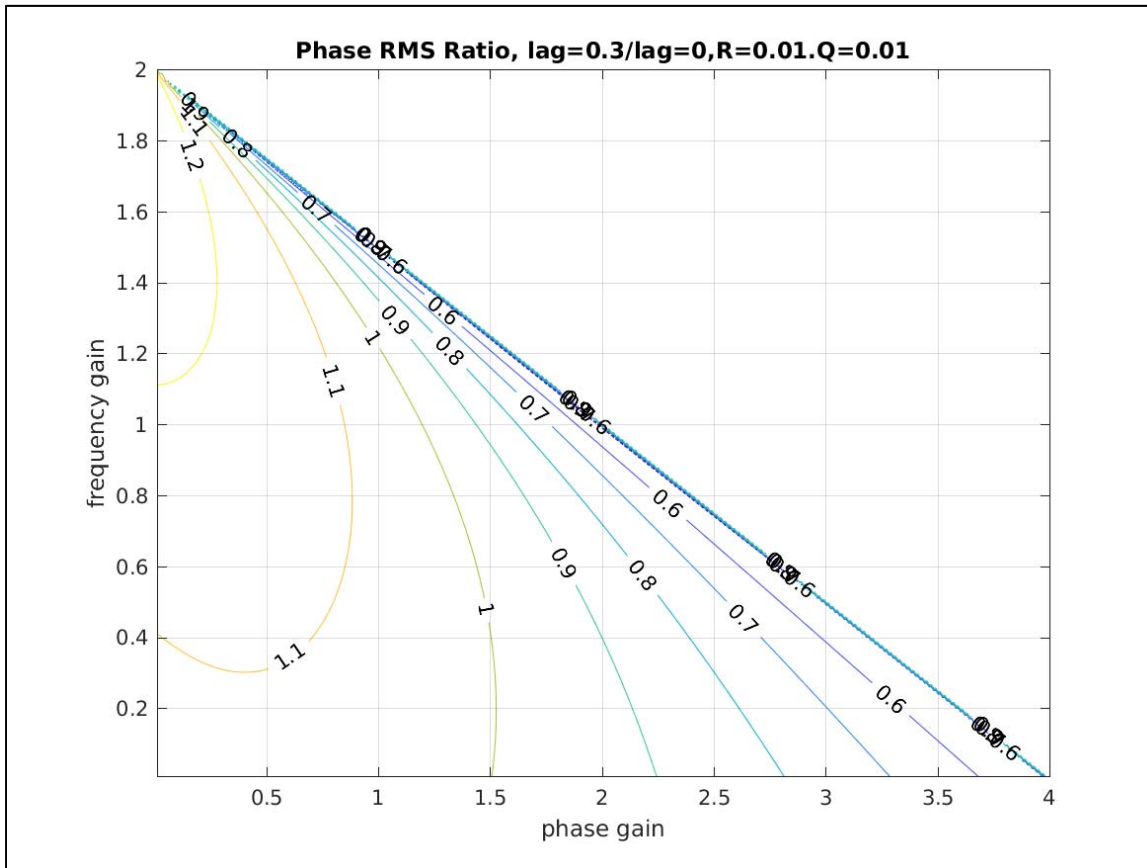


Figure 7.1 Ratio of phase RMS when steers are implemented later than measurements by 30% of the measurement interval, to the RMS when the steers are immediately implemented.

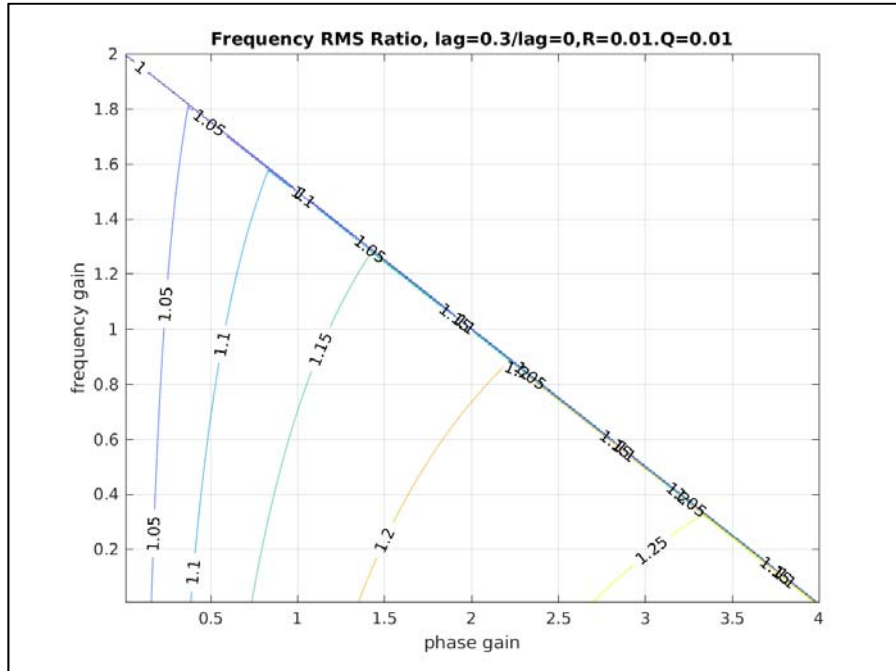


Figure 7.2 Ratio of frequency RMS when steers are implemented later than measurements by 30% of the measurement interval, to the RMS when the steers are immediately implemented.

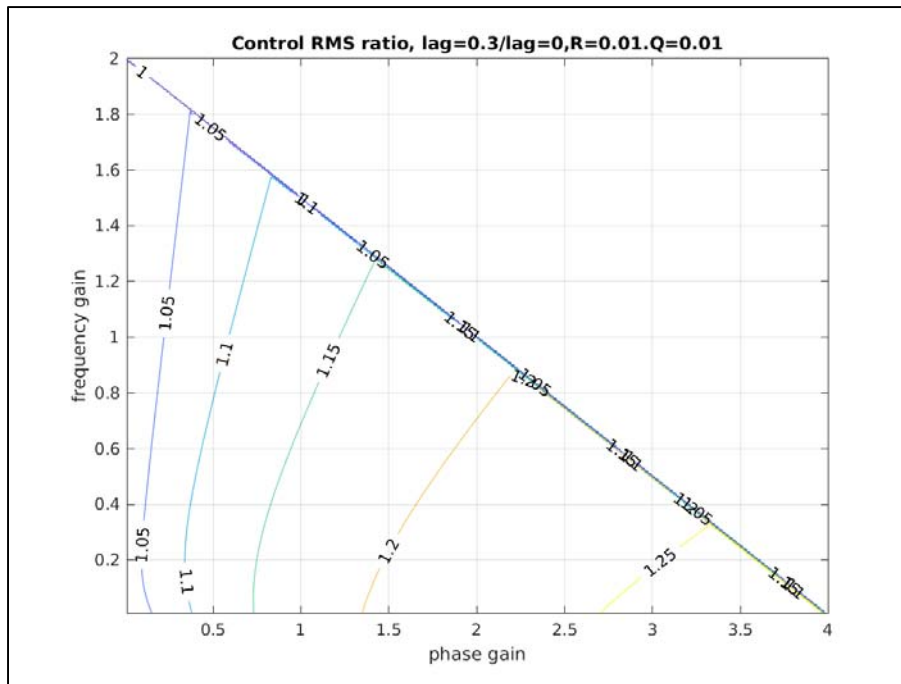


Figure 7.3 Ratio of control RMS when steers are implemented later than measurements by 30% of the measurement interval, to the RMS when the steers are immediately implemented.

When data are steered to UTC or UTC_r, the data come in batches and this analysis would be strictly correct if only the last datum of each batch were used. In such cases, the user may wish to use the intermediate points to estimate the final state, and apply either the LQG or PP approach to

determine what the phase and frequency of the state should be at the time when the next batch is slated to arrive. The actual steers could be those that would bring about that final state with the minimum amount of control, as in [10, 6]. This has been termed “gentle steering”.

VIII Conclusions

Although the need for simulations always remains, particularly for non-Gaussian behavior, the analytic techniques needed for a complementary analysis of the pole placement and linear quadratic approaches have been demonstrated. These allow estimates of the quantitative degradation due to suboptimal state estimation and delays in information transfer, such as the latency inherent in the monthly computations of UTC and weekly computations of UTCr.

IX. Disclaimer

The software package Matlab is mentioned for technical clarity and because other workers may find references to it to be useful. As a matter of policy, neither the US Naval Observatory nor the U.S. Government will endorse any commercial product.

X. References

- [1] N. Kalouptsides, 1997, “Signal Processing Systems Theory and Design”, John Wiley and Sons, Inc.
- [2] K. Ogata, 1995 ,”Discrete-Time Control Systems”, 2nd ed, Englewood Cliffs, NJ: Prentice-Hall
- [3] A. Locatelli, 2001, “Optimal Control an Introduction”, Birkhauser Verlag, Basel-Boston-Berlin
- [4] M. Athans, 1971, “The Role and Use of Stochastic Linear-Quadratic-Gaussian Problem in Control System Design,” IEEE Trans. Aut. Cont., AC-16,6, pp. 529-552
- [5] P. Koppang, D. Johns, and J. Skinner, 2004, “Application of Control Theory in the Formation of a Timescale” 35th Annual Precise Time and Time Interval (PTTI) Systems and Applications Meeting, pp 319-325
- [6] P. Koppang, 2016, “State space control of frequency standards”, Metrologia 83 R60-64
- [7] H.H. Rosenbrock and P.D. McMorran, 1971, “Good, Bad, or Optimal?”, IEEE Trans. Aut. Cont., AC-16,6, pp. 552-559
- [8] M.G. Safonov and M.K.H Fan, Editorial, International Journal of Robust and Nonlinear Control, 7, 97-103, 1997
- [9] T.D. Schmidt, M. Gödel, and J. Furthner, "Investigation of Pole Placement Technique for Clock Steering," Proceedings of the 49th Annual Precise Time and Time Interval Systems and Applications Meeting, Reston, Virginia, January 2018, pp. 22-29.
- [10] P. Koppang and D. Matsakis, “New Steering Strategies for the USNO Master Clock”, Proceedings of the 31th Annual Precise Time and Time Interval Systems and Applications Meeting, pp. 277-284.

Appendix 1. The Allan variances, given the steering gain function G , measurement noise R , and process noise Q

In our scalar notation, the Allan variance is defined as

$$\sigma_y^2(n\tau) = \frac{1}{2n\tau} < (p_{k+2n} - 2p_{k+n} + p_k)^2 > = \frac{1}{2} < (f_{k+n} - f_k)^2 > \quad (\text{A1.1})$$

Returning to the vector notation we note that:

$$x_{k+1} = (\Phi - BG)x_k + K_g z_{k+1} \quad (\text{A1.2})$$

$$x_{k+n} = (\Phi - BG)^n x_k + \sum_{m=1}^n (\Phi - BG)^{n-m} K_g z_{k+m} \quad (\text{A1.3})$$

$$x_{k+2n} = (\Phi - BG)^{2n} x_k + \sum_{m=1}^{2n} (\Phi - BG)^{2n-m} K_g z_{k+m} \quad (\text{A1.4})$$

$$(x_{k+2n} - 2x_{k+n} + x_k) = (I - (\Phi - BG)^n)^2 x_k + \sum_{m=1}^{2n} (\Phi - BG)^{2n-m} K_g z_{k+m} - 2 \sum_{m=1}^n (\Phi - BG)^{n-m} K_g z_{k+m} \quad (\text{A1.5})$$

$$(x_{k+2n} - 2x_{k+n} + x_k) = (I - (\Phi - BG)^n)^2 x_k + \sum_{m=n+1}^{2n} (\Phi - BG)^{2n-m} K_g z_{k+m} - \sum_{m=1}^n [2(\Phi - BG)^{n-m} - (\Phi - BG)^{2n-m}] K_g z_{k+m} \quad (\text{A1.6})$$

Realizing that the Allan variance is computed using only the phase components.

$$2n\tau\sigma_y^2(n\tau) = < [(x_{k+2n} - 2x_{k+n} + x_k)(x_{k+2n} - 2x_{k+n} + x_k)^T] > \quad (\text{A1.7})$$

Terms involving x_k and $z_{k'}$ are correlated only if $k'=k$, and defining

$$N = < (K_g z_k)(K_g z_k)^T > = K_g (H Q H^T + R) K_g^T = N^T \quad (\text{A1.8})$$

$$2n\tau\sigma_y^2 = (I - (\Phi - BG)^n)^2 \Sigma_x (\Phi - BG)^n + \sum_{m=n+1}^{2n} (\Phi - BG)^{2n-m} N (\Phi - BG)^{2n-m,T} + \sum_{m=1}^{n-1} [2(\Phi - BG)^{n-m} - (\Phi - BG)^{2n-m}] N [2(\Phi - BG)^{n-m} - (\Phi - BG)^{2n-m}]^T \quad (\text{A1.9})$$

The Allan Variance of the frequency steers is found by multiplying the gain vector times the difference between x_k and equation A1.3's expression for x_{k+n} with the transpose of that product:

$$2\sigma_{y,steers}^2(n\tau) = G [I - (\Phi - BG)^n] \Sigma_x [I - (\Phi - BG)^{n,T}] G^T + G \sum_{m=1}^n (\Phi - BG)^{n-m} N (\Phi - BG)^{n-m,T} G^T \quad (\text{A1.11})$$

All of these expressions can be easily though tediously coded on a computer.

Appendix II. Figures illustrating the mapping between gains, poles, and decay constants.

The figures in this appendix show the decay times, frequencies, and polar distances associated with every possible stable pair of gains, and the gains that would result from all possible pole positions within the unit circle.

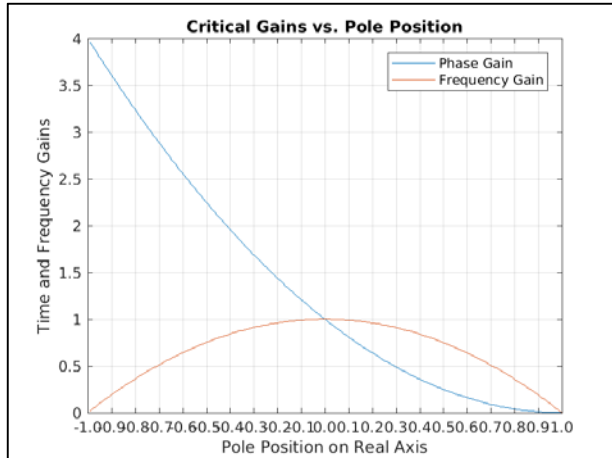


Figure A.1. Critical phase and frequency gains as function of pole position. Gains exceeding 1.0 are not recommended.

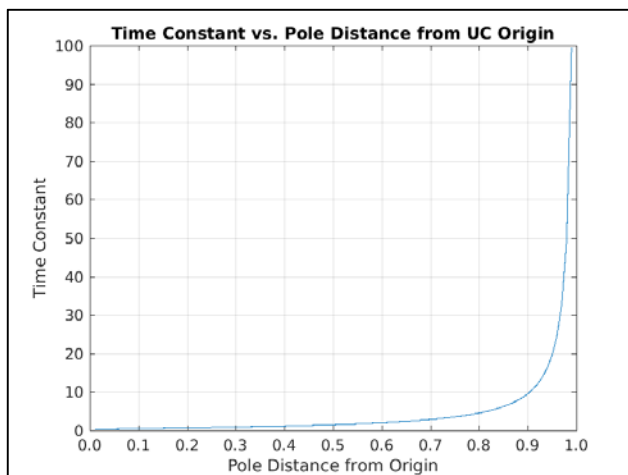
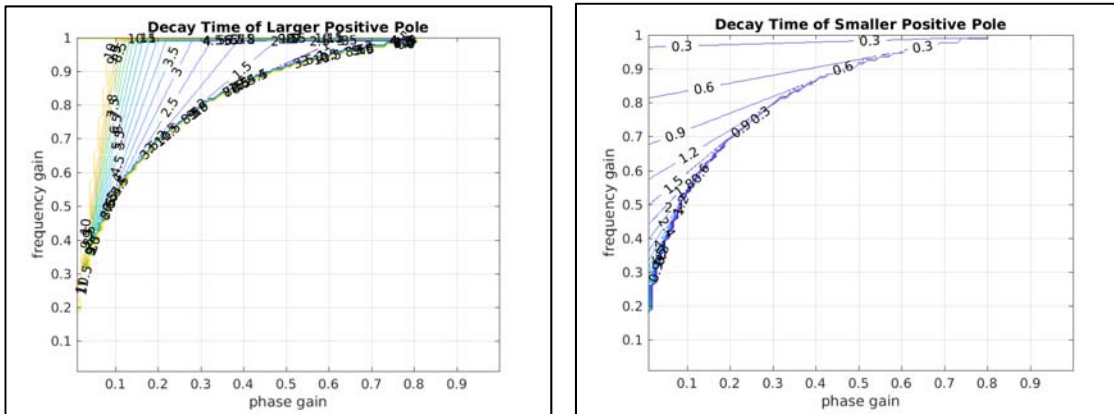


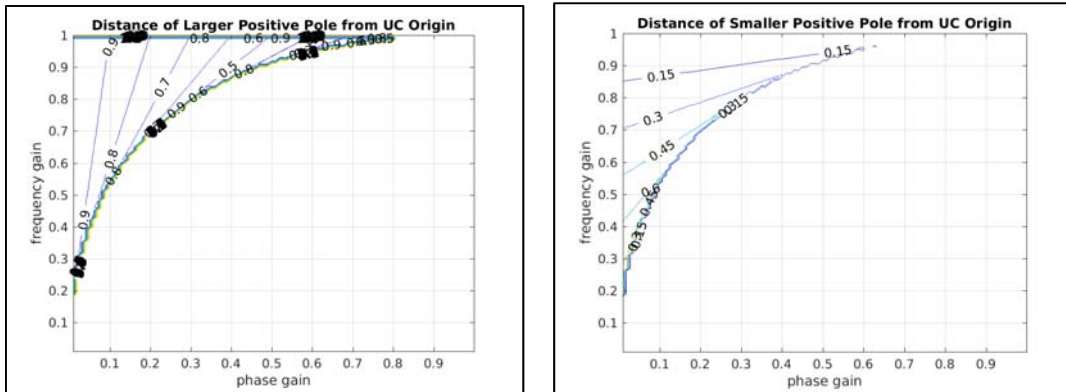
Figure A.2. Time constant as function of the pole's distance from the origin of the unit circle

Figures A-3 to A-6. Positions and decay times of pole configurations on gain-gain plots:

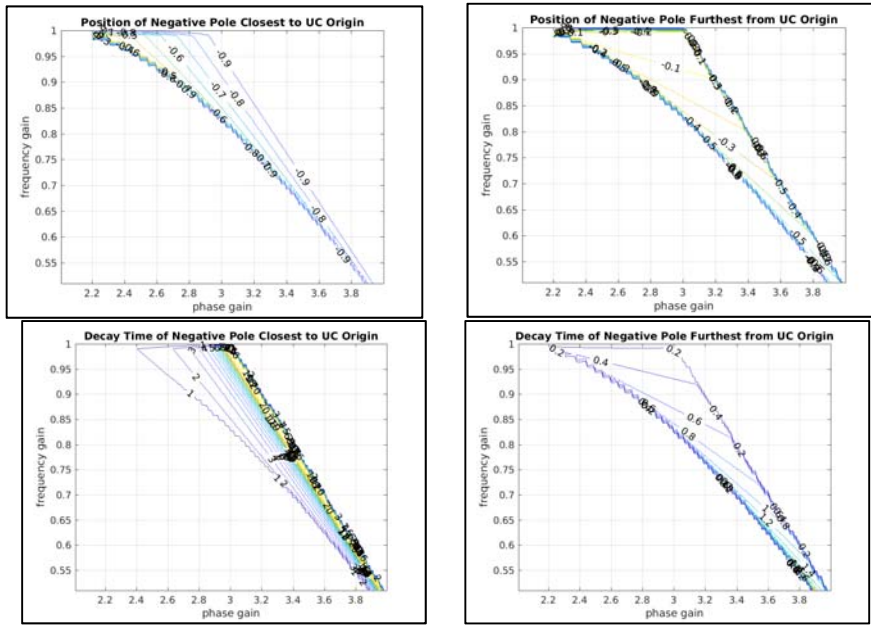
Decay times of two positive poles:



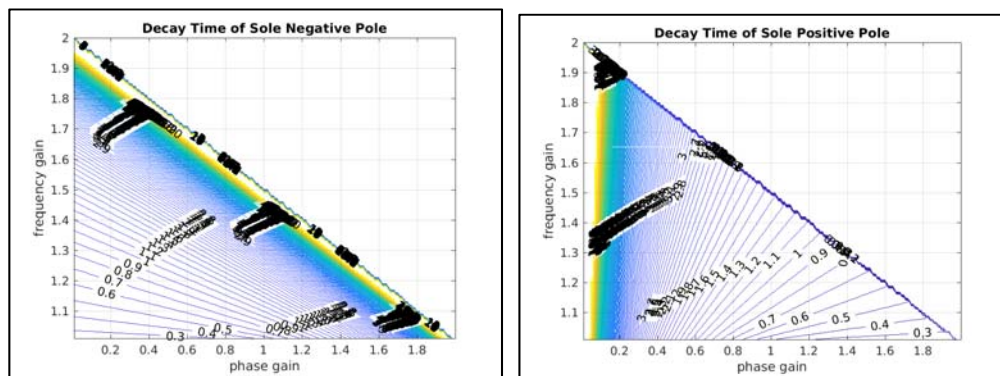
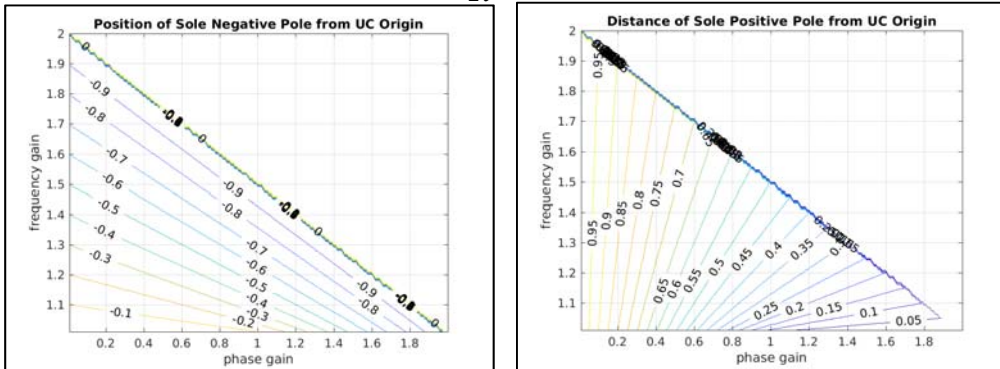
Positions of two positive poles:



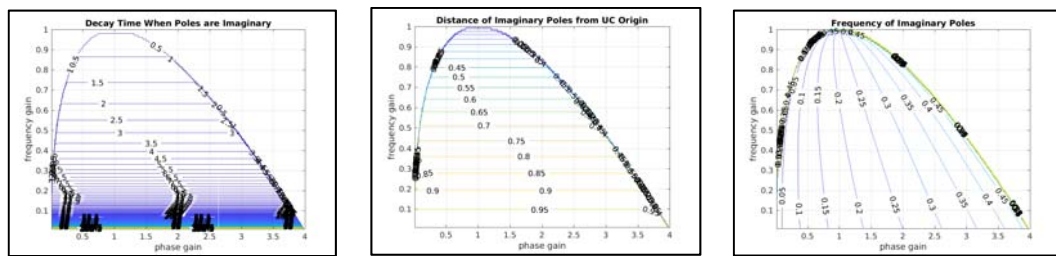
Figures A-7 to A-10 Decay times when there are two negative poles. All negative poles are oscillatory, $f_{osc} = \frac{1}{2\tau}$



Figures A-11 to A-14. Decay times and polar radii when there is one negative and one positive pole. The negative pole is oscillatory $f_{osc} = \frac{1}{2\tau}$

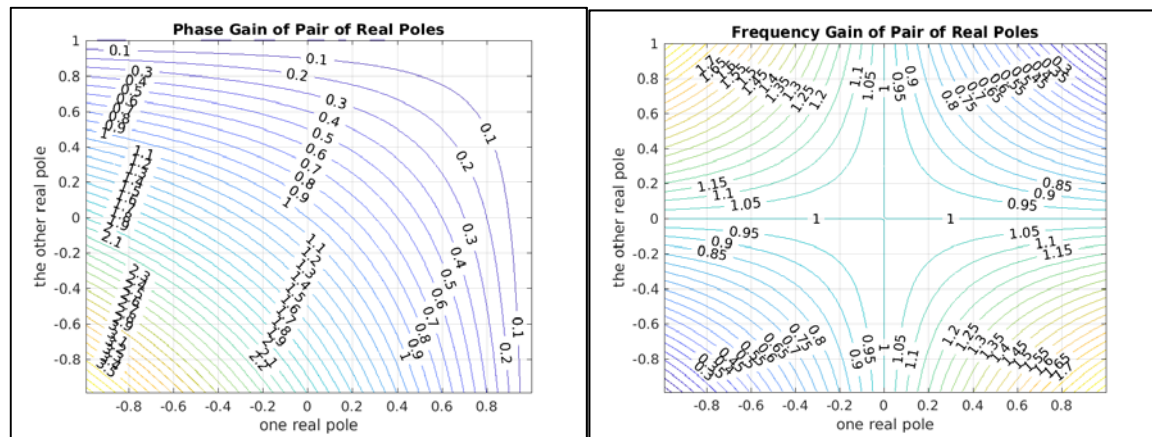


Figures A-15 to A-17 Decay times and frequencies of when there are (conjugate) imaginary poles. The frequencies are in units of $1/\tau$

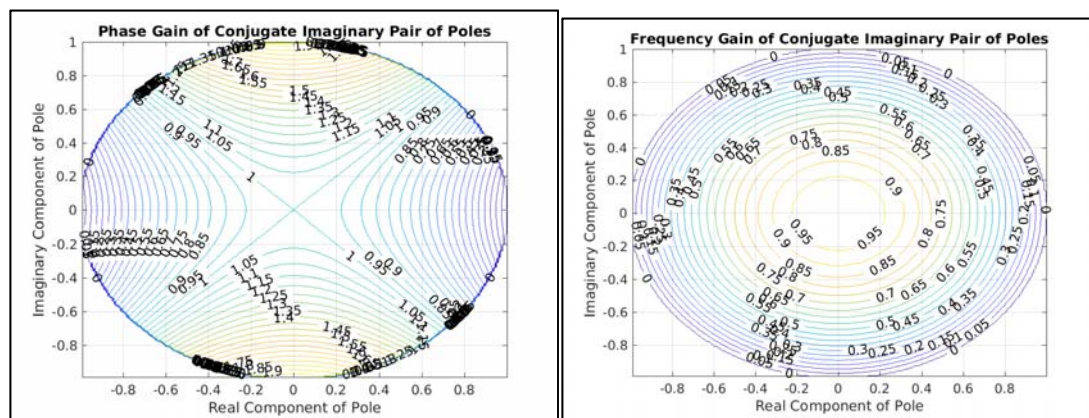


Figures A-18 to A-

19 Phase and frequency gains as function of positions of pairs of real poles



Figures A-20 to A-21 Phase and frequency gains as function of positions of pairs of conjugate imaginary poles.



Appendix III. The statistics for suboptimal state estimating when the frequency gain is unity.

With reference to section vi, the Sylvester equation 6.12 cannot be solved when $g_2=1$, because the matrix $A = \begin{pmatrix} 1-g_1 & 0 \\ -g_1 & 0 \end{pmatrix}$ is singular. But it is possible to solve the system of equations directly, using the following:

$$KH = \begin{pmatrix} 1 & 0 \\ 1 & 0 \end{pmatrix}; I - KH = \begin{pmatrix} 0 & 0 \\ -1 & 1 \end{pmatrix}; \Phi(I - KH)^T = \begin{pmatrix} 1 & 1 \\ 0 & 1 \end{pmatrix} \begin{pmatrix} 0 & -1 \\ 0 & 1 \end{pmatrix} = \begin{pmatrix} 0 & 0 \\ 0 & 1 \end{pmatrix} \quad (\text{A3-1})$$

If a, b, c, and d the components of $\Sigma_{x_{\Delta x}}$, while e, f, g, and h are the components of the last two terms of 6.11:

$$\Sigma_{x_{\Delta x}} = \begin{pmatrix} a & b \\ c & d \end{pmatrix} = \begin{pmatrix} 1-g_1 & 0 \\ -g_1 & 0 \end{pmatrix} \begin{pmatrix} a & b \\ c & d \end{pmatrix} \begin{pmatrix} 0 & 0 \\ 0 & 1 \end{pmatrix} + \begin{pmatrix} e & f \\ g & h \end{pmatrix} \quad (\text{A3-2})$$

$$\Sigma_{x_{\Delta x}} = \begin{pmatrix} a & b \\ c & d \end{pmatrix} = \begin{pmatrix} 1-g_1 & 0 \\ -g_1 & 0 \end{pmatrix} \begin{pmatrix} 0 & b \\ 0 & d \end{pmatrix} + \begin{pmatrix} e & f \\ g & h \end{pmatrix} \quad (\text{A3-3})$$

$$\Sigma_{x_{\Delta x}} = \begin{pmatrix} a & b \\ c & d \end{pmatrix} = \begin{pmatrix} 0 & (1-g_1)b \\ 0 & -g_1b \end{pmatrix} + \begin{pmatrix} e & f \\ g & h \end{pmatrix}; \begin{pmatrix} a & g_1b \\ c & d+g_1b \end{pmatrix} = \begin{pmatrix} e & f \\ g & h \end{pmatrix} \quad (\text{A3-4})$$

Redefining a, b, c, d, e, f, g, and h to their analogous values to solve 6.4, we obtain:

$$\Sigma_x = \begin{pmatrix} a & b \\ c & d \end{pmatrix} = \begin{pmatrix} 1-g_1 & 0 \\ -g_1 & 0 \end{pmatrix} \begin{pmatrix} a & b \\ c & d \end{pmatrix} \begin{pmatrix} 1-g_1 & -g_1 \\ 0 & 0 \end{pmatrix} + \begin{pmatrix} e & f \\ g & h \end{pmatrix} \quad (\text{A3-5})$$

$$\Sigma_x = \begin{pmatrix} a & b \\ c & d \end{pmatrix} = \begin{pmatrix} 1-g_1 & 0 \\ -g_1 & 0 \end{pmatrix} \begin{pmatrix} (1-g_1)a & -g_1a \\ (1-g_1)c & g_1c \end{pmatrix} + \begin{pmatrix} e & f \\ g & h \end{pmatrix} \quad (\text{A3-6})$$

$$\Sigma_x = \begin{pmatrix} a & b \\ c & d \end{pmatrix} = \begin{pmatrix} (1-g_1)^2a & -g_1(1-g_1)a \\ -g_1(1-g_1)a & g_1^2a \end{pmatrix} + \begin{pmatrix} e & f \\ g & h \end{pmatrix} \quad (\text{A3-7})$$

$$a = (1-g_1)^2a + e \quad ; \quad a = e/(1 - (1-g_1)^2) = e/(2g_1 - g_1^2) \quad (\text{A3-8})$$